INVESTIGATING CELLULAR FUNCTIONS OF THE *SMARCAD1* GENE IN HUMAN MPNST CELLS BY CRISPR-CAS13D KNOCKDOWN

by

Han Han

A Thesis

Submitted to the Faculty of Purdue University

In Partial Fulfillment of the Requirements for the degree of

Master of Science

Department of Comparative Pathobiology

West Lafayette, Indiana

May 2022

THE PURDUE UNIVERSITY GRADUATE SCHOOL
STATEMENT OF COMMITTEE APPROVAL

Dr. GuangJun Zhang, Chair
Department of Comparative Pathobiology

Dr. Suresh Mittal
Department of Comparative Pathobiology

Dr. Timothy L. Ratliff
Department of Comparative Pathobiology

Approved by:
Dr. Sanjeev K. Narayanan

This thesis is dedicated to my parents.

ACKNOWLEDGMENTS

First, I would like to thank my advisor Dr. GuangJun Zhang for offering me this great opportunity to work in his lab. I appreciate all the guidance he has given to me during the time I was in the graduation program. He not only gave me so many suggestions regarding academia, but he also offered valuable advice about my life.

Second, I would like to express my gratitude to Dr. Timothy Ratliff, who has provided important advice during every important step of my graduate study. I will always appreciate him for his support and patience.

I am also very grateful to Dr. Suresh Mittal for serving on my committee. He and his lab have provided me with so many important resources. It is impossible for me to finish my research without help from him.

TABLE OF CONTENTS

LIST OF TABLES 7
LIST OF FIGURES 8
ABSTRACT 9
1. INTRODUCTION 10
1.1 MPNST 10
1.1.1 Epidemiology of MPNST 10
1.1.2 Pathology of MPNST 10
1.1.3 MPNST Etiology 11
1.1.4 Management of MPNSTs 13
1.2 The SMARCAD1 gene 15
1.2.1 Functions of SMARCAD1 15
1.2.2 DNA damage repairing functions of SMARCAD1 16
1.2.3 Smarcad1 is a tumor suppressor gene 17
1.3 CRISPR- Cas13d gene knockdown system 18
1.3.1 Gene knockdown technologies 18
1.3.2 Classification of CRISPR-Cas system 19
1.3.3 CRISPR-Cas13d is an advanced gene knockdown system 20
2. MATERIAL AND METHODS 22
2.1 Cell lines and cell culture 22
2.2 CRISPR-Cas13 SMARCAD1 knockdown in HEI193 cells 22
2.2.1 gRNA array design 22
2.2.2 DNA Construct Generation 22
2.2.3 Transformation and plasmid construct diagnosis 23
2.2.4 Generating a stable cell line 23
2.2.5 Verification of SMARCAD1 knockdown in the CRISPR-Cas13d HEI193 cell line 24
2.3 Western blotting 24
2.4 DNA damage repair response 25
2.5 Cell viability and anchorage-independent growth 26
3. RESULTS 28

3.1 SMARCAD1 expression in human Schwann and MPNST cells..... 28
3.2 Created SMARCAD1 knockdown Schwannoma cell line by CRISPR-Cas13d 29
3.3 Functional validation of SMARCAD1 Cas13d Knockdown cells by cell proliferation and anchorage-independent growth assays..... 30
3.4 Knockdown of SMARCAD1 compromises DNA damage repair in vitro and in vivo 31
4. DISCUSSION..... 34
4.1 CRISPR-Cas13d is an efficient gene knockdown system 34
4.2 Knockdown of SMARCAD1 causes cell growth inhibition..... 34
4.3 SMARCAD1 involves in the DNA damage repair process..... 35
REFERENCES 36

LIST OF TABLES

Table 1. Sequences of gRNA oligos 27

LIST OF FIGURES

Figure 1. Functions of SMARCAD1..... 18

Figure 2. Illustration of CRISPR-Cas13d system: Cas13d protein is capable to process its own CRISPR array with multiple gRNAs. Cas13d will identify specific mRNA sequences with the guidance of gRNAs. Then target mRNA sequence will be cleaved by Cas13d's RNase activity. It will lead to mRNA degradation eventually. 21

Figure 3. Tet-on CRISPR-Cas13d expression system constructs. Doxycycline-inducible SMARCAD1 knockdown system contains two constructs: pLentiRNACRISPR_007 will express Cas13d after being induced by doxycycline **(above)**. pLentiRNACRISPR_001 harbors a crRNA array having three spacers with their direct repeats **(below)**. 27

Figure 4. SMARCAD1 expression in human Schwann and MPNST cells. **A)** The expression level of SMARCAD1 in six human MPNST cell lines and, one immortalized human benign Schwannoma cell line HEI-193. **B)** SMARCAD1 expression level of 4 human neurofibroma and two Schwann cell lines (all harboring *NF1* mutations except HEI193) and ipn02.3 2λ, an immortalized human normal Schwann cell line..... 29

Figure 5. High knockdown efficiency of SMARCAD1 by CRISPR-Cas13d. CRISPR-Cas13d SMARCAD1 knockdown HEI193 cells **(A)** and shRNA SMARCAD1 knockdown HEI193 cells **(B)** were treated with different dosages (125, 250, 500, 1000, and 2000 ng/ml) of doxycycline. Western blots were performed to measure SMARCAD1 expression after 3-days of doxycycline-induced knockdown. 30

Figure 6. Cell proliferation and anchorage-independent growth were suppressed in the CRISPR-Cas13d SMARCAD1 cell line. A) 5-days cell proliferation of SMARCAD1 knockdown HEI193 cells was measured by MTT assay. **B)** Colony numbers of Cas13d SMARCAD1 knockdown Schwannoma cells were counted in soft-agar assay. DOX-: cells without doxycycline treatment. DOX+: cells with doxycycline treatment (500ng/ml for MTT assay; 100ng/ml for soft-agar assay) 31

Figure 7. The Loss function of SMARCAD1 compromises DNA damage repair *in vitro* and *in vivo*. A) γH2AX expression was examined by western blot in CRISPR-Cas13d SMARCAD1 knockout HEI193 cell line after 4Gy X-ray irradiation. **B)** γH2AX expression was examined by western blot in wildtype, *smarcad1a*$^{sa1299-/-}$, and *smarcad1a*$^{p403-/-}$ 1dpf zebrafish embryos. **C)** Quantification of γH2AX expression measured by western blotting from A. Relative fold change of γH2AX were calculated upon each collecting time point after irradiation. Bars are the means of three independent experiments in same time point. Student's *t*-test was performed to caluate the significance between wildtype and two zebra fish mutants (SA1299 and p403) (*: $p \leq 0.05$; **: $p \leq 0.01$; ***: $p \leq 0.001$; NS: $p > 0.05$) 32

ABSTRACT

Malignant Peripheral Nerve Sheath Tumor (MPNST) is a form of soft tissue sarcoma arising from peripheral nerve sheath cells. Currently, there is no clinically available targeted therapy because the targetable essential driver genes in this tumor are largely unknown. SMARCAD1 (SWI/SNF-related, matrix-associated actin-dependent regulator of chromatin, subfamily A, containing DEAD/H box 1) has been identified as a new tumor suppressor of MPNSTs in zebrafish. Several studies have also linked *SMARCAD1* with cancer development together. However, the cellular roles of *SMARCAD1* in human MPNST cells remain unclear. To investigate DNA damage repair functions of SMARCAD1 in human MPNST, we created a doxycycline-inducible Schwannoma cell line by CRISPR-Cas13d, a newly developed mRNA knockdown method. I verified efficiently SMARCAD1 knockdown cell line by western blot. In addition, knockdown of SMARCAD1 inhibits Schwannoma cell proliferation and anchorage-independent growth. It is reported that SMARCAD1 is involved in DNA damage repair mechanisms. I confirmed that loss of SMARCAD1 expression compromises DNA damage repairing function in Schwannoma cells. This result was also verified in two zebrafish *smarcad1* mutants. In summary, I utilized a novel gene knockdown approach to generate a SMARCAD1 Schwannoma cell line and validated its function in DNA damage repair. This study might provide information for developing a new treatment option for MPNSTs.

1. INTRODUCTION

1.1 MPNST

1.1.1 Epidemiology of MPNST

Malignant Peripheral Nerve Sheath Tumor (MPNST) is a form of soft tissue sarcoma arising from peripheral nerve sheath cells (Schwann cells) (Louis et al., 2016). It is an aggressive tumor that tends to invade surrounding normal tissues. Although it is not a type of common cancer with an incidence rate of 1.46 per million individuals in the US (Bates et al., 2014), MPNSTs account for around 10% of all types of soft tissue sarcomas (Fuchs et al., 2005; Czarnecka, 2018). It also has a poor 5-year survival rate between 16 and 52% (Natalie Wu & Lu, 2019). Approximate 50% of all MPNST cases are observed in patients with neurofibromatosis type 1 (NF1) (Amirian et al., 2014), which is an autosomal-dominant genetic disorder caused by the *NF1* gene mutation. MPNSTs are one of the most common non-rhabdomysosarcomatous soft tissue sarcomas diagnosed in children (Amirian et al., 2014). Although peak diagnosis ages are 30-40 years among the NF1-affected population, 70-80 years are the peak ages for the general population, and pediatric cases still account for 10-20% of all MPNSTs.

1.1.2 Pathology of MPNST

MPNSTs often occur on the limbs and trunk, and they are also found in other body regions like the head and neck (Kar et al., 2006). Diagnosis is difficult for MPNST due to the lack of specific histology characteristics and immunohistochemistry markers (Combemale et al. 2014). Thus, over the years, other types of soft tissue sarcomas have been incorrectly identified as MPNSTs (Allison et al., 2005; Inoue et al., 2014). Sarcoma arising from a pre-existing benign nerve sheath tumor should be qualified as MPNST (Ferrari et al., 2007). For example, malignant tumors with a spindle cell morphology identified in neurofibromatosis type 1 patients should be considered as MPNST unless proven otherwise. Sarcoma involved in a major nerve should be highly suspected as MPNST, whereas several MPNST mimics should not be excluded as well, such as synovial sarcoma, rhabdomyosarcoma, leiomyosarcoma, or angiosarcoma (Allison et al., 2005). Tumors with no major nerve-relate are the most challenging type for MPNST diagnosis. It

requires tests combining morphology examination and immunohistochemistry detection for the Schwann cells.

Morphologically, MPNST cells are spindled, hypercellular tumor cells with intersecting fascicles. Other morphologic features such as perivascular accentuation of cellularity, tumor herniation into vascular lumens and necrosis are frequently found in this type of tumor (Rodriguez et al., 2012). Several immunohistochemical features of MPNST can be utilized for the diagnosis. S100 is a non-specific marker that separates neural crest origin tumor cells from non-neural neoplasms (Kuberappa, 2016). It expresses in around 50% of MPNST cases but usually with a scattered pattern (Stasik & Tawfik, 2006), which is significantly different from diffused expression patterns in Schwannoma or melanoma (Thway & Fisher, 2014). Therefore, usage of S100 immunostaining provides a crucial diagnostic criterion to distinguish MPNST from other MPNST mimics such as Schwannoma and different types of soft tissue sarcomas. Positive staining of other common IHC markers, including CD34 and SOX10 been utilized for MPNST diagnosis, although they cannot separate MPNST from Schwannoma and neurofibroma (Naber et al., 2011; Miettinen et al., 2015). Recent studies revealed that loss of H3K27me3 can be used for sensitively identifying MPNST (Prieto-Granada et al., 2016; Cleven et al., 2016; Sugita et al., 2021). 72% of all MPNST cases showed completely loss of H3K27me3 expression, and 23% of all patients have a partial loss pattern (Prieto-Granada et al., 2016). However, H3K27me3 cannot distinguish MPNST from melanoma because more than half of melanoma cases showed partial loss (Le Guellec et al., 2017). Overall, diagnosis of MPNSTs is difficult due to the lack of specific markers for distinguishing this type of tumor from its mimics.

1.1.3 MPNST Etiology

MPNST could sporadically occur or transform from the existing benign tumor, NF1 neurofibromas and Schwannomas that are linked with the *NF1* genes. The *NF1* gene encodes neurofibromin protein. It activates GTPase which dephosphorylates RAS-GTP into inactive RAS-GDP, therefore, suppressing the RAS signaling pathway (Martin et al., 1990). Loss of function of *NF1* gene lead to hyperactivation of RAS, which activates downstream pathways such as mTOR or MEK/MAPK pathways (Bergoug et al., 2020). These pathways contribute to cell viability, proliferation, and cell death. Loss of function of *NF1* results in benign neurofibroma formation,

but it is not sufficient for MPNST development (Yang et al., 2008). Other than *NF1*, somatic mutation of *CDKN2A*, *SUZ12*, *EGFR,* and *TP53* are frequently found in MPNSTs (Perry et al., 2002; Legius et al., 1994; De Raedt et al., 2014; M. Zhang et al., 2014). Loss of CDKN2A has been reported in the majority of atypical neurofibromas, which were identified as a precursor of MPNST (Beert et al., 2011; Chaney et al., 2020). However, alterations of *TP53*, *EGFR*, and *SUZ12* expression were only discovered in MPNST, not in benign or atypical neurofibromas (Legius et al., 1994; De Raedt et al., 2014; M. Zhang et al., 2014). These studies suggest a model that loss of *NF1* causes benign neurofibroma formation, then *CDKN2A* loss transfer benign neurofibroma to premalignant neurofibroma. In contrast, alterations of *TP53*, *EGFR*, and *SUZ12* only contribute to the malignant transformation of MPNST (Prudner et al., 2020).

Besides mutations of tumor driver genes, DNA copy number alterations (CNAs) are reported in MPNSTs. Cytogenetic studies using array comparative genomic hybridization (aCGH) identified copy number gains on chromosomes 7, 8q, 15q, and 17q, and losses on 1p, 9p, 11, 12p, 14q, 17q, 18, 22q, X, and Y in human MPNSTs (Beert et al., 2011). Deletion of human chromosome locus 9p21.3 was most observed in this comparative study. This region harbors the *MTAP*, and *CDKN2A/B* genes, which are reported to involve in different types of tumors. The most identified gains are on 5q14.1, 7p14.1 and 7q36.1, which contain the *AP3B1*, *CUL1,* and *NEDL1* genes (Mantripragada et al., 2009). These genes were reported to function as cell cycle regulators, which may provide advantages for cancer cell growth.

Naturally, there are many key tumor driver candidates of MPNST, whereas it is difficult to identify them within these large CNAs. Zhang et al. narrowed down the number of tumor driver candidates by cross-species comparisons between humans and zebrafish. The rationale behind this approach is: first, similar to human MPNST, zebrafish MPNST has been identified as highly aneuploid. Secondly, many essential cancer genes, including *tp53*, *pten*, *nf1*, and *nf2* are conserved between these two species (Berghmans et al., 2005; Faucherre et al., 2008; Rudner et al., 2011; Shin et al., 2012). Thirdly, the evolutionarily distance between humans and zebrafish is far, which means they share small syntenies. The locations of genes on chromosomes have been reshuffled during evolution (Postlethwait et al., 1998). Therefore, the passenger genes can be excluded more efficiently through this comparison. Many genes, such as *CCND2, ETV6, HGF, HSF1, KIT, MDM2, MET,* and *PDGFR*, were identified gained in both humans and zebrafish. These genes have previously been found overexpressed in a variety of human tumors. Three genes that are

frequently lost in human Schwann cell tumors: *NF1*, *NF2*, and *SMARCB1,* are also found in copy number loss regions both in human and zebrafish samples. *PTEN* is a key tumor suppressor gene which has been identified lost in both humans and zebrafish. The dosage of PTEN expression was identified to controls the development neurofibroma and the malignant transformation into MPNSTs (Gregorian et al., 2009). Some novel tumor suppressors, such as *SMARCAD1*, *LZTR1, SMARCA2, and KANK1,* were identified as lost (G. Zhang et al., 2013). This study has screened various oncogene/ tumor suppressor gene candidates in MPNST. It also demonstrated the genetic complexity of MPNSTs due to their aneuploidy.

1.1.4 Management of MPNSTs

Management of MPNST is challenging, and treatment option is limited. Similar to other types of soft tissue sarcoma, surgical resection is the first choice to treat MPNST. R0 resection with at least 2 centimeter extra excision around the tumor has the best outcome for the patients (Baehring et al., 2003). However, resection can be difficult depending on tumor size, location, and metastatic presentation. MPNSTs mainly develop along major nerves. The most common sites involved in MPNSTs are extremities. The trunk, head, and neck are common locations (Kar et al., 2006). Therefore, R0 resection for extremities MPNSTs relatively results in better outcomes compared to head and neck MPNSTs (Ferrari et al., 2002). However, resection for the tumors involved in local vascular would potentially result in necrosis. Resection for head and neck MPNSTs is extremely challenging and usually results in a poorer outcome (Knight et al., 2022). Re-resection is recommended if primary resection is unable to remove the tumor completely. Adjuvant radiation therapy can be performed to improve local control for large high-grade lesions (>5cm) (Angelov et al., 1998). Generally, MPNSTs have a high recurrence rate after surgery, which can be 40-65% (Du et al., 2019). More studies are required to improve surgical management of this type of tumor.

Traditional chemotherapy has a minimal response by most MPNST patients (Bradford & Kim, 2015). Doxorubicin and ifosfamide have been considered the most effective chemotherapeutic reagents, which were either treated solely or combinedly (Seno et al., 2017). The study has shown that NF1-associated MPNSTs have fewer responses to chemotherapy compared with sporadic MPNSTs (Higham et al., 2017). Radiation therapy should be used with

caution for NF1-related MPNST since radiation is one of the triggers for the malignant transformation of type-1 neurofibroma (Evans et al., 2006). Targeted therapies are generally highly potent and with fewer side effects. Thus, the development of targeted therapy is crucial for treating this type of tumor**.** However, clinical trials for these inhibitors haven't achieved promising results yet, though many attempts have been made in the past. Ras signaling pathway has been considered targetable in NF1-associated MPNST because the biallelic mutation of the *NF1* gene hyperactivates RAS protein. Tipifarnib, a farnesyl protein transferase inhibitor that inhibits post-translational farnesylation of RAS protein, has been observed with no objective responses in phase I trial in pediatric neurofibroma patients (Widemann et al., 2006). RAS signaling downstream, MAPK pathway is a potential target as well. The MEK inhibitor, PD184352, was reported to selectively induce MPNST cells apoptosis (Mattingly et al., 2006). However, currently, there is no clinical data available to prove it is effective in patients. Sorafenib, a small molecular inhibitor of VEGF and RAF, indicated a promising non-progression rate in patients with different types of metastatic sarcomas. However, the phase II trial failed in MPNST patients (Maki et al., 2009). Similarly, clinical trials for inhibitors against mTOR, PTEN, and EGFR were still ongoing (Farid et al., 2014), but no promises were seen. Therefore, currently, there is no targeted therapy clinically available for MPNST because the key driver genes in this tumor are largely unknown.

DNA replication and DNA damage repairing pathway genes have been revealed as potential targets for MPNST therapy. Topoisomerase IIα (*TOP2A*) was identified highly upregulated in MPNSTs but not in neurofibromas by cDNA microarray analyses (Skotheim et al., 2003). It was reported that the response of *TOP2A* inhibitor etoposide was improved in MPNST patients with the combination of ifosfamide (Higham et al., 2017). Poly-ADP ribose polymerase inhibitors (PARPi) target DNA damage repairing mechanism. They are widely used in treating different types of cancer including ovarian cancer, prostate cancer, and BRCA1/2 deficient breast cancer. Kivlin et al. found that PARP1 and PARP2 have high expression levels in MPNST tissue samples. PARP inhibitor AZD2281 effectively suppresses proliferation in multiple MPNST cell lines. AZD2281 treatment also decreases cell proliferation and increases cell apoptosis of MPNST xenograft (Kivlin et al., 2016). These studies suggest genes involved in DNA replication and damage repairing could potentially be a therapeutic target if there is a synthetic lethality effect in cancer cells.

1.2 The *SMARCAD1* gene

1.2.1 Functions of SMARCAD1

Human chromosome fragment 4q22-23 was reported to be deleted in MPNST and several other types of cancer (Adra et al., 2000; Cetin et al., 2008; Uzunoglu et al., 2014). To identify MPNST driver genes in this chromosomal region, our lab analyzes copy number alteration (CNA) in human MPNSTs and zebrafish MPNSTs by massively parallel sequencing. The *SMARCAD1* (SWI/SNF-related, matrix-associated actin-dependent regulator of chromatin, subfamily A, containing DEAD/H box 1) gene has been identified as a tumor suppressor candidate in the 4q22-23 region (G. Zhang et al., 2013). SMARCAD1 belongs to the SNF2 protein family that remodels chromatin using energy from ATP hydrolysis (Schoor et al., 1999). We recently have demonstrated that a homologous zebrafish gene, *smarcad1a*, is a novel tumor suppressor gene for zebrafish MPNSTs (Han et al., 2022).

The function of this gene and its orthologs are not extensively studied yet in mammalian cells, but based on yeast studies on its homologous gene, *FUN30,* and sporadic studies in human cell lines and invertebrates, SMARCAD1 has three main functions **1). It controls gene expression.** Fission yeast *smarcad1* ortholog FUN30^{FFT3} was found to disassemble nucleosomes in transcriptional regions to promote RNA Polymerase lI transcription (Lee et al., 2017). Drosophila SMARCAD1 protein was reported to enhance the acetylation of histone H2A K5 and K8 through interaction with CREB-binding protein (CBP), resulting in transcription activation (Doiguchi et al., 2016). Yeast Fun30 was also reported to regulate alternative RNA splicing (Niu et al., 2020) **2). SMARCAD1 maintains heterochromatin and regulates DNA replication.** Rowbotham et, al. reported that *SMARCAD1* knockdown increases acetylation of H3 and H4 and decreases methylation of H3K9, suggesting SMARCAD1 maintains heterochromatin. In addition, it was found to interact with histone deacetylases (HDACs), H3K9 methyltransferase G9a, and heterochromatin maintenance factor KRAB-associated protein 1 (KAP1) in maintaining heterochromatin after DNA replication (Rowbotham et al., 2011). Another recent study has revealed that SMARCAD1 transfers the whole histone octamer between DNA segments ATP-dependently during de novo nucleosome assembly. Its catalytic activity requires the N-terminal tails of histone H3 and H4 (Markert et al., 2021). Moreover, heterochromatin maintained by *SMARCAD1* was reported to play an essential role in genome stability by inhibiting endogenous

retroviral elements (Sachs et al., 2019). Serval other studies have shown that SMARCAD1 interacts with DNA clamp PCNA protein (Proliferating Cell Nuclear Antigen) at the DNA replication site (Rowbotham et al., 2011; Yu & Maria, 2021). It was reported to prevent the accumulation of 53BP1 (p53-Binding Protein 1) and ATAD5 (ATPase Family AAA Domain Containing 5) in the replication site, therefore, maintaining PCNA level in replication folk in MRC5 human fibroblasts (Yu & Maria, 2021). **3). SMARCAD1 is involved in the DNA damage repairing mechanism.** SMARCAD1 plays essential roles in multiple DNA damage responses such as DNA mismatch repair pathway (MMR) (Terui et al., 2018) and homologous recombination (HR) induced by double-strand DNA breaks (DSB) (Chakraborty et al., 2018; Costelloe et al., 2012; Densham et al., 2016). SMARCAD1 was reported to involve in double-strand break (DSB) repairing pathway choice and required for DNA end-resection (Costelloe et al., 2012). In addition, SMARCAD1 promotes homologous recombination by removing 53BP1 on the DNA DSB site (Densham et al., 2016).

1.2.2 DNA damage repairing functions of SMARCAD1

There are two major double strand break repairing pathway: Homologous recombination (HR) and Non-homologous end-joining (NHEJ). Homologous recombination is an error-proof DSB repairing pathway that only processes during the G1 and S phases due to its requirement for homologous DNA. DNA end-resection is an important step in HR. This process generates a 3' single-stranded DNA overhang that can "invade" the homologous sequence to eventually restore the break site. SMARCAD1 was reported to promote DNA end-resection. Knockdown of SMARCAD1 reduced ssDNA generation at the DSB site in human osteosarcoma cell lines (Chakraborty et al., 2018; Costelloe et al., 2012). Decreased localizations of HR proteins such as RPA, RAD51, and BRCA1 at the DSB site were also observed after SMARCAD1 knockdown (Chakraborty et al., 2018). These results indicate that SMARCAD1 has an essential role in DSB repairing choice, but the mechanism is still unclear.

Interestingly, 53BP1, a DSB repairing pathway choice regulator, was found to be removed late from DSB sites in *SMARCAD1* knockdown cells (Chakraborty et al., 2018). 53BP1 is a chromatin reader that identifies and binds to H4K20me2 and H2AK15ub to facilitate NHEJ and limits DSB end-resection (Fradet-Turcotte et al., 2013; Wilson et al., 2016).

The yeast *smarcad1* ortholog *fun30* (function unknown number 30) was reported to facilitate DNA end-resection. *Fun30* deletion bubble yeast showed a slower resection rate than the wild type after DSB. However, in yeast *53BP1* ortholog *rad9* knockout mutant, *fun30* becomes less important in DNA resection than in wildtype bubble yeast (Chen et al., 2012). This result suggests *fun30* facilities DNA end-resection by overcoming inhibition from *rad9*. Densham et al. confirmed a similar mechanism in human cells by double knockdown of *53BP1* and *SMARCAD1*. Double knockdown recovered the suppression of DNA end-resection caused by single knockdown of *SMARCAD1* (Densham et al., 2016). Several discoveries have suggested SMARCAD1 promotes DNA end-resection by remodeling 53BP1 targeting histone through its histone-transfer ability. However, the detailed mechanism of SMARCAD1 facilitating DNA end-resection by antagonizing 53BP1 function is still unclear.

1.2.3 *Smarcad1* is a tumor suppressor gene

Human *SMARCAD1* has been found frequently lost in MPNST and several other types of cancers. Many studies have linked *SMARCAD1* with cancer development together. Mutation of a skin-specific isoform of SMARCAD1 has been found in human squamous cell carcinoma (Günther et al., 2018). Knockdown of *SMARCAD1* in breast cancer cells leads to decreased cell migration proliferation and metastasis (Al Kubaisy et al., 2016). Homozygous *Etl1* (Mouse *SMARCAD1* ortholog) knockout mice experience serval abnormalities, including gastro-intestinal tumors (Schoor et al., 1999). As previously described, *SMARCAD1* maintains heterochromatin and DNA break repair pathways, and both are critical for suppressing tumor development.

Our recent data show that loss of *smarcad1a*, one of the orthologs of human *SMARCAD1* in zebrafish, accelerates tumorigenesis of MPNST with *tp53* mutation background (Han et al., 2021). This result provides genetic evidence to prove *smarcad1a* is a novel tumor suppressor gene in zebrafish. It is the first direct evidence to support *SMARCAD1*'s tumor suppressive function in vivo. However, whether human SMARCAD1 has a similar cellular function in Schwann and MPNST cells is still unknown.

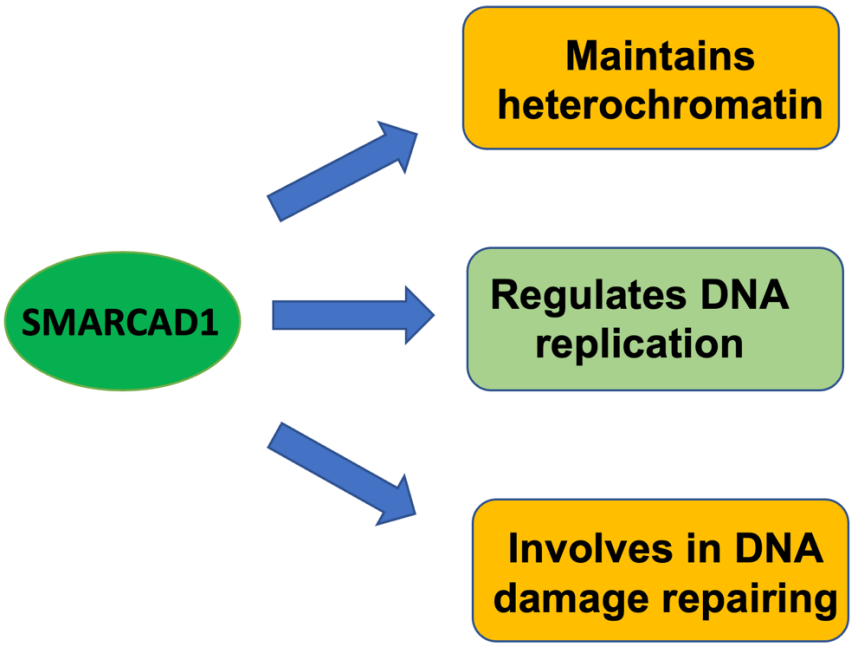

Figure 1. Functions of SMARCAD1

1.3 CRISPR- Cas13d gene knockdown system

1.3.1 Gene knockdown technologies

Inactivation of tumor suppressor genes usually promotes tumor development. Thus, knockdown/knockout of a potential tumor suppressor gene in premalignant/ benign tumor cells is an initial step to studying the tumor-suppressive suppressor gene's functions in cancer. There are several technologies developed for this purpose. RNA interference (RNAi) is an extensively used method for knockdown target gene. It contains two categories: transient expression of siRNA and stable expression of shRNA. siRNA (small interfering RNA) is a 21-23 base pair double-stranded RNA which is designed to target specific mRNA sequences (Bernstein et al., 2001). siRNA can be transfected into cancer cells to degenerate target mRNA associated with RNA-induced silencing complex (RISC) (Nykänen et al., 2001). However, gene knockdown by siRNA is temporary. The interference will be lost with cell division. The shRNA (short-hairpin RNA) is a stable siRNA delivery method. It is designed by adding a 19bp stem-loop structure to double-stranded siRNA.

shRNA can be assembled with Polymerase III promoters such as U6 in a construct and delivered into cells by a viral infection (Brummelkamp et al., 2002). Once transcript, shRNA will be processed by DICER into a siRNA, downregulating the target gene. RNAi is relatively highly efficient, and it is a powerful tool for studying tumor suppressor genes. However, studies have demonstrated that RNAi might interfere with multiple mRNAs other than the sequences they were designed to. This off-target effect can lead to a false conclusion when observing phenotypes after target gene knockdown (Putzbach et al., 2017). Moreover, the efficiency of RNAi is varied and highly dependent on the target sequence, while the mechanism of siRNA intracellular processing remains largely unclear.

Other technologies, such as CRISPR-Cas9, ZFNs, and TALENs, are DNA editing methods that will alter the cell genome permanently. CRISPR-Cas9 is a widely used technology due to its simplicity, effectiveness, and efficiency. However, these DNA-targeted methods have some drawbacks. These methods are highly relied on DNA damage repairing mechanism, which will bring a variety of mutations in the target gene. Therefore, isolation and characterization of individual mutants are necessary but also tedious steps while using these technologies. It is also challenging to study the genes of interest when such genes are essential for cell survival by these approaches.

In this study, we chose a newly developed CRISPR-Cas13d system, which is a highly sensitive RNA-editing knockdown tool for generating SMARCAD1 loss-of-function cell lines.

1.3.2 Classification of CRISPR-Cas system

CRISPR-Cas system was first identified in E. coli. It functions as an adaptive immunity against mobile genetic elements like viruses in bacteria. One of the defense activities of CRISPR-Cas systems is sequence-specifically DNA/RNA cleavage guided by RNA (Mohanraju et al., 2016). All the currently discovered CRISPR-Cas systems have been separated into two classes. Class 1 system functions by forming protein complex that contains multiple Cas proteins, whereas class two functions only use a single protein with multiple functional domains (Makarova et al., 2015). Because the class 2 Cas system contains less elements, it has been widely adopted as a genome editing tool (Cong et al., 2013; Hsu et al., 2014; Wright et al., 2016). Class 2 CRISPR-

Cas systems have been classified into three types, II, V and VI. Type VI systems are the only known RNA-targeting CRISPR system so far.

1.3.3 CRISPR-Cas13d is an advanced gene knockdown system

CRISPR-Cas13 is an RNA-guided, RNA-targeting CRISPR-Cas system (Type VI) that has been recently identified and utilized for mRNA knockdown (Abudayyeh et al., 2017; O'Connell, 2019). Similar to Cas9, Cas13 forms a complex with guide RNA that contains a short hairpin and around 30nt spacer. It recognizes the hairpin and targets a specific RNA sequence complementary to the spacer sequence. Cas13's RNase activity leads to cleavage of the target transcript (O'Connell, 2019). As Cas13 can cleavage crRNA array into gRNAs, this feature allows us to target multiple sequences at the same time using a crRNA array that is composed of gRNAs (Abudayyeh et al., 2017). So far, four subtypes of Cas13 have been discovered, including Cas13a, Cas13b, Cas13c, and Cas13d (Shmakov et al., 2017; Konermann et al., 2018). Similar to PAM (protospacer adjacent motif) sequence for Cas9, efficiently RNA cleavage by Cas13a/b/c requires a protospacer flanking site (PFS) in the targeted RNA sequence, which is a specific single nucleotide at the 5' or 3' end of the guide RNA. Cas13d, however, can facilitate RNA knockdown in mammalian cells PFS-independently (Konermann et al., 2018). Therefore, the gRNA design for Cas13d has fewer limitations. The Figure 2 illustrates the progress of CRSIPR-Cas13d knockdown. Cas13d from *Ruminococcus flavefaciens* XPD3002 (CasRfx) has been identified with robust activity in human cells. It was proved to have better knockdown efficiency than shRNA, CRISPRi, and other Cas13s (Konermann et al., 2018). I used this novel RNA knockdown system in studying the functions of SMARCAD1 in human cell lines in this study.

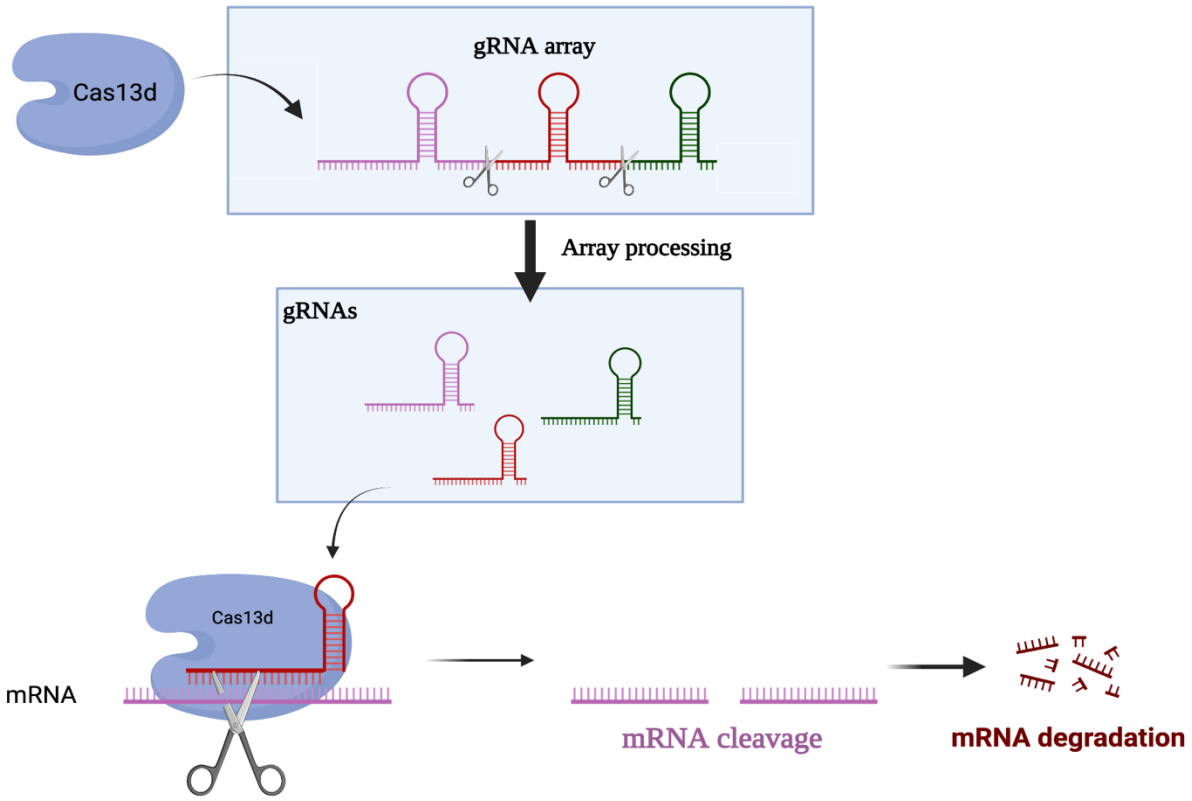

Figure 2. Illustration of CRISPR-Cas13d system: Cas13d protein is capable to process its own CRISPR array with multiple gRNAs. Cas13d will identify specific mRNA sequences with the guidance of gRNAs. Then target mRNA sequence will be cleaved by Cas13d's RNase activity. It will lead to mRNA degradation eventually.

2. MATERIAL AND METHODS

2.1 Cell lines and cell culture

The human MPNST cell lines, human kidney epithelial cell line HEK293T, and human schwannoma cell line HEI193 were purchased from ATCC. Cells were cultured in Eagle's minimal essential medium (DMEM) with 10% fetal bovine serum (FBS). Penicillin (100IU/ml), and streptomycin (100ug/ml) were added to the culture media during cell culture. All the cells were incubated at 37°C humidified incubator with 5% CO_2.

2.2 CRISPR-Cas13 SMARCAD1 knockdown in HEI193 cells

2.2.1 gRNA array design

To knockdown SMARCAD1 expression in a schwannoma cell line, we utilized a newly developed RNA targeting CRISPR-Cas13d system. The protein-coding transcript of SMARCAD1 was targeted. Cas13d was reported to have pre-crRNA processing ability. It can cleavage a gRNA array that targets different RNA sequences. We designed a crRNA array that contains three different gRNAs that target exon2, exon 12, and exon 24 (3'UTR), respectively, based on the sequence of the ENSEMBL transcript (ENST00000354268). The three gRNAs were designed with an online Cas13 design tool (https://cas13design.nygenome.org/). Sequences of gRNAs can be found in **Table 1**. The prediction suggests no off-targets for these gRNAs.

To assemble three gRNA into the RNA assay, we designed two oligos with restriction endonuclease cutting site (BsmB I), which contain three individual mRNA sequences **(Table 1).** All oligonucleotides were synthesized by the ITD (The Integrated DNA).

2.2.2 DNA Construct Generation

To express gRNAs and cas13d protein in HEI193 cells, we chose an established tetracycline-inducible Cas13d expression system (Wessels et al., 2020). It contains two constructs, pLentiRNACRISPR007-TetO-NLS-RfxCas13d-NLS-WPRE-EFS-rtTA3-2A-Blast and pLentiRNACRISPR001-hU6-RfxCas13d-DR1-BsmBI-EFS-Puro-WPRE. plentiRNA001

constantly expresses gRNAs, while plentiRNA007 expresses Cas13d protein only under doxycycline activation. **(Figure 3)**

We ligated two oligos containing gRNAs sequence with plentiCRISPRRNA001 vector using golden gate cloning (K. Zhang et al., 2020). First, the sense strand and antisense strand oligonucleotides were annealed in a thermocycler using a thermocycler program: 95°C: 5 minutes, 95-85°C: -20°C /second, 85-25°C: - 0.10°C /second. Next, we mixed two double-stranded oligonucleotides (2ul each oligonucleotide) with 300ng plentiCRISPRRNA001 empty vector and then added 1ul Type IIS endonuclease BsmB I (New England Biolabs, #R0739L) and 1ul T4 ligase (New England Biolabs, #M0202M). The reactions were incubated in a thermocycler with a thermocycler program: (42°C: 1min, 16°C) X 60, 60°C: 5min, 12°C, 2min.

2.2.3 Transformation and plasmid construct diagnosis

We performed plasmids transformation using the heat shock method (Hanahan, 1983). Five microliter ligation product was added into 50ul of competent E. coli cells stbl3. The mixture was incubated on ice for 30min. Then, heat shock was performed by incubating E. coli cells at 42 for 1min, then transferred to ice and incubated for 2min. Next, 150ul LB media was added to the mixture, and sample tubes were incubated in an orbital cell culture shaker at 37°C. All the products will be spread onto an LB agar plate with 50ug/ml ampicillin. The transformed cells were incubated overnight at 37°C to produce enough colonies.

Colony PCR was performed to identify colonies with the correct plasmid. Forward primer SV40pA-F (5'-GGACAAACCACAACTAGAATGCAG-3') and reverse primer U6a-Seq333F (5'-GCTCTCCCTCCAGCTCTTGGTTC-3') were used to identify the inserted sequence in plentiCRISPRRNA001 vector. Colonies with positive PCR band will be cultured overnight at 37°C. Mini-prep was performed to extract the plasmid then the correct plasmid will be verified by Sanger-sequencing.

2.2.4 Generating a stable cell line

A stable SMARCAD1 knockdown HEI193 cell line was chosen because it has relative normal SMARCAD1 expression by western blot, and it is a benign tumor cell line. First, plentiRNACRISPR007, a doxycycline inducible Cas13d expression construct, was transduced into

the HEI193 cell line by lentivirus. HEK293T cell line was used to produce lentivirus by transient transfection. About 10ug plentiRNACRISPR007 construct, 7.5ug lentivirus packaging construct CMV-DR8.2 and 2.5ug lentivirus envelop construct CMV-VSVG were transfected together into HEK293T cells using Turbofect (Thermo Fisher, # R0531) transfection reagent following the manufacturer protocol. The cell culture medium was refreshed after overnight incubation. Then media containing lentivirus was collected twice at 48hr and 72hr post-transfection. This medium was filtered and concentrated by LentiX concentrator according to the manufacturer's manual. After further concentrated by centrifugation, all the viruses were used to infect HEI193 cells. Cells were incubated with viruses and 8ug/ml polybrene overnight, then incubated in fresh cell culture media for 24hr. 5ug/ml blasticidin was used to select positive cells for at least seven days.

Next, the plentiRNACRSIPR001 construct containing three gRNA was introduced into plentiRNACRISPR007-HEI193 cells, which conditionally express Cas13d. The procedure of lentiviral transduction followed the protocol described above. plentiRNACRSIPR001 construct has a puromycin resistance element instead of a blasticidin resistance element. Therefore, 2ug/ml puromycin was used to select cells that express both Cas13d and gRNAs.

2.2.5 Verification of SMARCAD1 knockdown in the CRISPR-Cas13d HEI193 cell line

Newly generated Tet-on Cas13d SMARCAD1 knockdown HEI193 cells were seeded into a 6-well plate. Different dosages of doxycycline (0, 125ng, 250ng, 500ng, 1000ng, 2000ng/ml) were treated in each well through serial dilutions. After three days of treatment, cells were collected and lysed. Then cell lysates were used to detect SMARCAD1 expression by western blot following the procedure that will be described in 2.3.

2.3 Western blotting

Treatment for each sample before western blot is different dependent on different experiment designs. Cells were incubated and cultured until 80% confluency. Then cell samples were lysed by ice-cold RIPA buffer with a protease inhibitor (Roche: #5892791001) and a phosphatase inhibitor (Roche: #4906837001) directly after being rinsed three times with cold PBS. Bicinchoninic acid (BCA) assay was used to measure the total protein concentration in each sample using a kit (Thermo Fisher, #23227). Total protein was electrophoresed on SDS-page gels

with different concentrations, depending on the target protein size. Then proteins were transferred to the PVDF membrane to perform blotting (Bio-rad # 1620177). Antibodies used for western blot: human Anti-phosphorylated-histone H2A.X (Ser139) (Millipore, 05-636; 1:1000), zebrafish Anti-phosphorylated-histone H2A.X (Ser139) (Genetex, GTX127342; 1:1000), anti-SMARCAD1 (#12458, Cell signaling: 1:1000), β-ACTIN (sc-47778, Santa Cruz, 1:2000). Images were taken using Azure 280 Economical Chemi Imager (Azure, #AZI280). Band/protein intensity was quantified using ImageJ software.

2.4 DNA damage repair response

Human Schwannoma cell line HEI193 with doxycycline induced *SMARCAD1* knockdown and without *SMARCAD1* knockdown were treated with 4Gy X-ray irradiation. The radiation was produced with an X-ray irradiator (X-RAD 320, PXi Precision X-Ray) with a dose rate of 1 Gy/25s. Cells were then lysed using RIPA buffer with 10% protease inhibitor (Roche: #5892791001) and 10% phosphatase inhibitor (Roche: #4906837001) at 30min, 60min, 120min, 600min post-irradiation. BCA assay was used to measure the total protein concentration in each sample. Western blots were performed following the procedure described in section 2.3.

Zebrafish embryos were raised in Petri dishes with system water and 0.01mg/L methylene blue until 1-day post- fertilization. Before irradiation, chorions were removed by incubating fish embryos in fish water with 1mg/mL pronase. Then pronase was washed out, and embryos were rinsed with fish system water 3 times. Then the de-chlorinated embryos were resting in system water for at least one hour. Next, embryos were treated with 15Gy X-ray irradiation with a dose rate of 1 Gy/25s. Non-irradiated control embryos were mock irradiated at room temperature as well. All Embryos were collected for protein extraction at 1hour, 24 hours, 36 hours, 48 hours, and 72 hours post-irradiation. At each collection point, embryos were transferred into 1.5mL Eppendorf tubes. System water was removed then 1mL deyolking buffer (0.3 mM PMSF and 10 mM EDTA in calcium-free Ringer's solution) was added to each tube. The yolk was removed by gently pipetting up and down, followed by a brief centrifuge (200 rpm, 30 seconds). After removing the yolk, embryos were rinsed in calcium-free Ringer’s solution three times to completely remove the yolk. Then RIPA lysis buffer with a protease inhibitor cocktail (Roche: #5892791001) and a phosphatase inhibitor (Roche: #4906837001) was added to completely lysis

embryos. BCA assay was used to measure the total protein concentration in each experiment sample. Western blots were performed following the procedure in section 2.3.

2.5 Cell viability and anchorage-independent growth

The cell viability of the *SMARCAD1* knockdown HEI193 cell line was measured by MTT assay. Cas13d SMARCAD1 knockdown HEI193 cell line was seeded in a 96-well plate. Two thousand cells were seeded in each well. On the second day, doxycycline (500ng/ml) was added to half of the wells to induce SMARCAD1 knockdown. 24 hours later, all the wells were treated with MTT (3-(4,5-Dimethylthiazol-2-yl)-2,5-diphenyltetrazolium bromide (Thermo #M6494, 0.5 mg/ml). Viable cells are capable of reducing MTT into insoluble formazan. After 4 hours of incubation, cell media was removed. 100ul DMSO was added into each well to dissolve formazan. A plate spectrophotometer (Bio-TEK) was used to measure optical density at 595nm in each well. Cell viability will be tracked for 5 days. Student *t*-test was used to calculate the significance between non-doxycycline treatment and doxycycline treatment cells.

The soft-agar assay was performed to examine anchorage-independent growth in Schwannoma cells. Briefly, 1% and 0.6% agar were prepared and autoclaved prior to the experiment. Both agar solutions were cooled down in a water bath until the temperature dropped to 42°C. Then 1% agar was mixed with cell culture media in a 1:1 ratio, 1.5ml of the mixture was added to each well in a 6-well plate. The plate will be incubated at room temperature for 10min to let the agar solidify. HEI193 SMARCAD1 CRISPR-Cas13d cells were trypsinized and re-suspended in cell culture media. One thousand cells were seeded in each well. 0.6% agar was mixed with cells suspension in a 1:1 ratio. 1ml mixture with agar and cells was placed in each well on the top of lower agar layer. The plate will be incubated at room temperature for 10min to let the agar solidify. Then 1 ml cell culture media was gently added on the top of upper agar layer. The plate was incubated overnight in a 37°C humidified incubator. The next day, the media in the 3 wells on the first roll was changed into a medium containing 100ng/ml doxycycline. The media in other wells was changed into fresh culture media without doxycycline. The plate was incubated for 3 weeks to form colonies. The cell culture medium was refreshed twice weekly. After three weeks, colonies were stained with 1% of crystal violet, then images were token for counting colonies.

Table 1. Sequences of gRNA oligos

Oligo name	5'- Sequence-3'
SMARCAD1A-Cas13d1F	CGTCTCCAAACAACAACGATCAAATGAGGACCATAACCCCTACCAACTGGTCGGGGTTTGAAACCAGCAATATAGACTGACAGGAGACG
SMARCAD1A-Cas13d1R	CGTCTCCTGTCAGTCTATATTGCTGGTTTCAAACCCCGACCAGTTGGTAGGGGTTATGGTCCTCATTTGATCGTTGTTGTTTGGAGACG
SMARCAD1A-Cas13d2F	CGTCTCCGACAGGCAGAACCCCTACCAACTGGTCGGGGTTTGAAACACATATTGGTAGAAAGCACCACCTTTTTGGAGACG
SMARCAD1A-Cas13d2R	CGTCTCCAAAAAGGTGGTGCTTTCTACCAATATGGTTTCAAACCCCGACCAGTTGGTAGGGGTTCTGCCTGTCGGAGACG

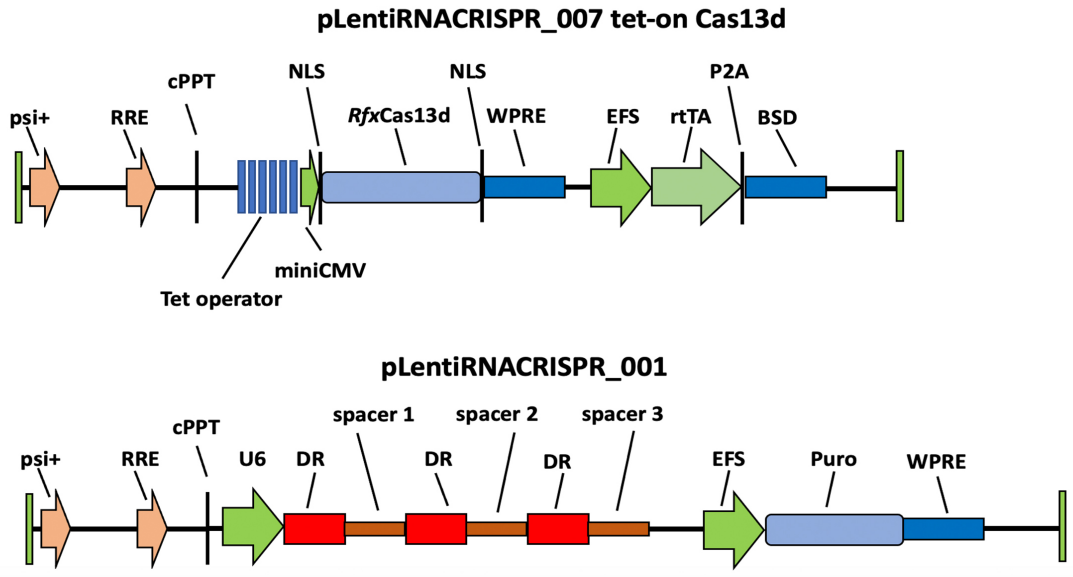

Figure 3. Tet-on CRISPR-Cas13d expression system constructs. Doxycycline-inducible SMARCAD1 knockdown system contains two constructs: pLentiRNACRISPR_007 will express Cas13d after being induced by doxycycline **(above)**. pLentiRNACRISPR_001 harbors a crRNA array having three spacers with their direct repeats **(below)**.

3. RESULTS

3.1 SMARCAD1 expression in human Schwann and MPNST cells

To study SMARCAD1 in human Schwannoma cells, first we need to knockdown the SMACAD1 in benign Schwannoma cells to observe the behavior changes involving in SMARCAD1 removal. Currently, there is no SMARCAD1 expression data available in human MPNST since it is rare cancer. To select available cell lines for functional study, we need to know SMARCAD1 expression in human MPNST and benign neurofibroma, and relative normal Schwann cell lines. I examined the SMARCAD1 protein level of six human MPNST cell lines and one schwannoma, cell line by western blot. The expression level of SMARCAD1 has been detected and quantified **(Figure 4A, B)**. SMARCAD1 is expressed at a low level in most MPNST cell lines compared with benign schwannoma cell line HEI193. Expression in sNF02.2, 90-8TL, and STS26T cells are significantly downregulated, while in sNF96.2, ST8814, and T265 cells, SMARCAD1 shows a mildly reduced expression (**Figure 4A**). These results are consistent with the SMARCAD1 tumor suppressor function in human MPNST.

To better understand the relative normal expression of SMRCAD1, I also examined SMARCAD1 expression levels in 4 more neurofibromas and 2 *NF1* deficient Schwann cell lines. Four out of six cell lines have a significantly lower level of SMARCAD1 compared to non-tumorous Schwann cell line ipn02.3 (**Figure 4B**). All four Schwannoma cell line with low SMARCAD1 level are originated from neurofibromatosis type 1 patients, which contains somatic *NF1* gene mutations. Low SMARCAD1 level in *NF1*-Schwannoma cells suggests SMARCAD1 could also be involved in Schwannoma formation in NF1 patients.

According to my results, the benign schwannoma cell line HEI193 has a relatively normal SMARCAD1 expression. Thus, I chose this cell line for the SMARCAD1 functional studies in this project.

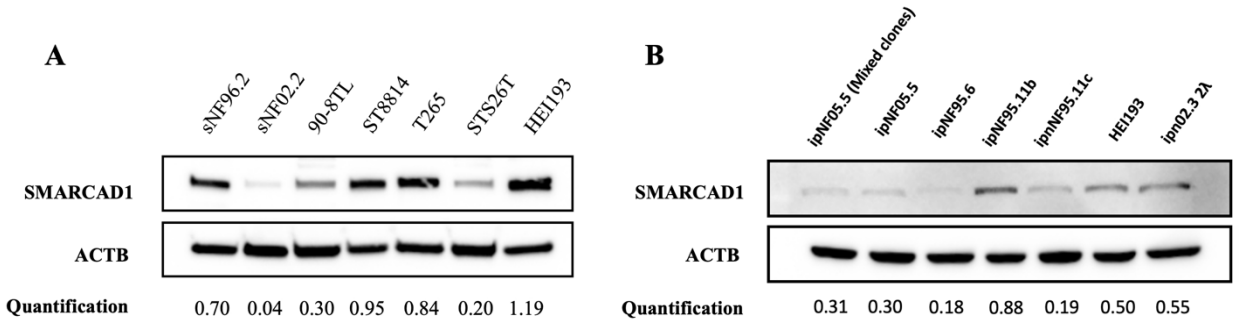

Figure 4. SMARCAD1 expression in human Schwann and MPNST cells. **A)** The expression level of SMARCAD1 in six human MPNST cell lines and, one immortalized human benign Schwannoma cell line HEI-193. **B)** SMARCAD1 expression level of 4 human neurofibroma and two Schwann cell lines (all harboring *NF1* mutations except HEI193) and ipn02.3 2λ, an immortalized human normal Schwann cell line.

3.2 Created SMARCAD1 knockdown Schwannoma cell line by CRISPR-Cas13d

To study the cellular functions of *SMARCAD1* in human Schwannoma and MPNST cells, I reasoned that loss-of-function is a suitable approach. Thus, I created a doxycycline-inducible SMARCAD1 knockdown HEI193 schwannoma cell line by CRISPR-Cas13d. The doxycycline system gives me the flexibility to adjust SMARCAD1 expression levels if needed. We choose knockdown SMARCAD1 in the HEI193 cell line, a benign Schwannoma cell line with relative normal SMARCAD1 expression level compared with normal Schwann cells **(Figure 4B)**. Western blot was performed to examine the knockdown efficiency and sensitivity toward doxycycline. Cells were treated with different dosages of doxycycline (0, 125ng, 250ng, 500ng, 1000ng, 2000ng/ml) for three days. Doxycycline was refreshed after 3 days of treatment. To verify that SMARCAD1 expression was knocked down successfully, I examined the treated stable cells using immunoblot. Indeed, the expression level of SMARCAD1 is significantly reduced (around 85% reduction) after doxycycline treatment at all concentrations of doxycycline treatment. **(Figure 5A)**. This result indicates a highly efficient SMARCAD1 knockdown in HEI193 cells by the tet-on cas13d binary knockdown system.

Our lab has already generated a SMARCAD1 knockdown HEI193 cell line using a commercial doxycycline-inducible shRNA construct (ULTRA-3351712, TransOMIC technologies Inc.) (Han et al., 2021). Thus, I compared the knockdown efficiency of Cas13d knockdown with shRNA knockdown by western blot. SMARCAD1 expression was also examined

after being treated with different dosages of doxycycline **(Figure 5B)**. SMARCAD1 has not been significantly downregulated (around 60% reduction) until cells were treated with no less than 500ng doxycycline in this shRNA knockdown cell line. In contrast, the CRISPR-Cas13d cell line is more sensitive toward doxycycline treatment and has better efficiency of SMARCAD1 knockdown.

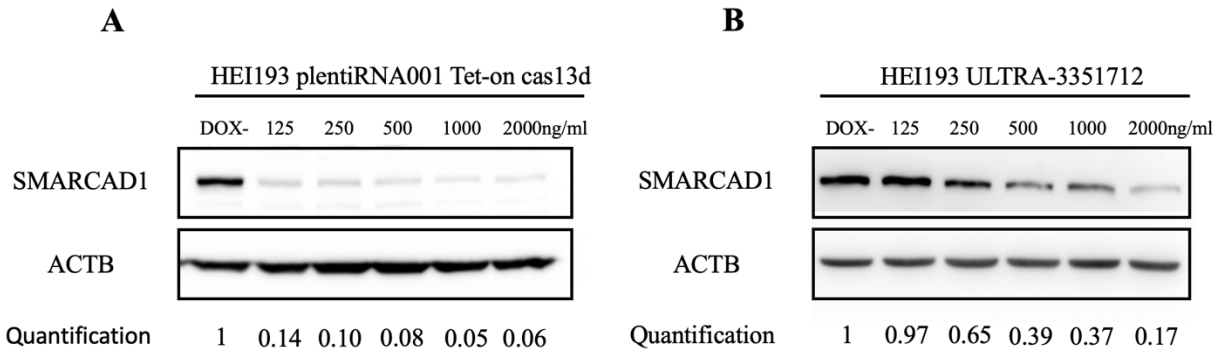

Figure 5. High knockdown efficiency of SMARCAD1 by CRISPR-Cas13d. CRISPR-Cas13d SMARCAD1 knockdown HEI193 cells **(A)** and shRNA SMARCAD1 knockdown HEI193 cells **(B)** were treated with different dosages (125, 250, 500, 1000, and 2000 ng/ml) of doxycycline. Western blots were performed to measure SMARCAD1 expression after 3-days of doxycycline-induced knockdown.

3.3 Functional validation of SMARCAD1 Cas13d Knockdown cells by cell proliferation and anchorage-independent growth assays

SMARCAD1 knockdown was reported to cause cell growth inhibition in xxx cells. In addition, we also verified this with HEI193 cells by shRNA knockdown (Han 2021). To further functionally validate this Cas13d knockdown cell line, I performed MTT and soft-agar assays. For the MTT assay, cells were separated into 500ng/ml doxycycline treatment and control groups. Cell number was continuously tracked by MTT assay for 5 days. Increased cell numbers can be observed in both treated and control groups. However, the cell growth of the SMARAD1-knockdown group was significantly suppressed comparing to the control group starting from the third day **(Figure 6A)**. This data indicates that knockdown of SMARCAD1 in Schwannoma cell line causes cell-growth delay. Moreover, anchorage-independent growth was significantly decreased after 21 days of incubation with 100ng/ml doxycycline **(Figure 6B)**. These results

indicate that knockdown by the CRISPR-Cas13d system effectively generates loss-of-function SMARCAD1 cells. In addition, these results also confirmed our previous findings on the growth defect caused by SMARCAD1 downregulation

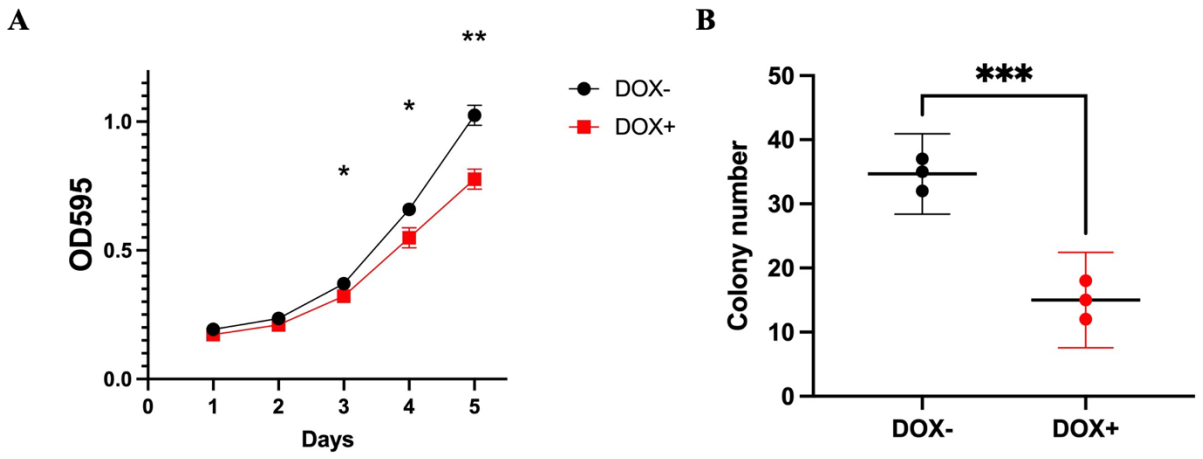

Figure 6. Cell proliferation and anchorage-independent growth were suppressed in the CRISPR-Cas13d SMARCAD1 cell line. A) 5-days cell proliferation of SMARCAD1 knockdown HEI193 cells was measured by MTT assay. **B)** Colony numbers of Cas13d SMARCAD1 knockdown Schwannoma cells were counted in soft-agar assay. DOX-: cells without doxycycline treatment. DOX+: cells with doxycycline treatment (500ng/ml for MTT assay; 100ng/ml for soft-agar assay)

3.4 Knockdown of SMARCAD1 compromises DNA damage repair in vitro and in vivo

Studies have suggested *SMARCAD1* has an important role in DSB repairing (Chakraborty et al., 2018; Costelloe et al., 2012). DNA double-strand breaks increase genomic instability, which will promote cancer development (Aparicio et al., 2014). Therefore, we reasoned that loss of *SMARCAD1* also compromises DNA damage repairing function in Schwannoma. I utilized the newly generated CRISPR-Cas13d SMARCAD1 knockdown Schwannoma cell line to test this hypothesis. SMARCAD1- knockdown cells and parental control cells were exposed to 4Gy X-ray irradiation to induce DNA double-strand breaks. Proteins were collected at a series of time points after irradiation. I chose to monitor DNA damage by γH2AX, a widely used surrogate marker for DNA damage. γH2AX stands for specificity phosphorylation in histone H2AX on the 139th serine residue. It can be rapidly activated by ataxia-telangiectasia mutated (ATM) protein kinase within

seconds after DNA damage occurs (Mah et al., 2010). Knockdown of SMARCAD1 leads to an elevated γH2AX level at 30min, 60min, and 120min post-irradiation compared to the control group **(Figure 7A)**, which indicates loss of SMARCAD1 reduces DSB repairing function in Schwannoma cells. This result suggests that the DNA damage repairing function of SMARCAD1 is involved in human Schwannoma cells.

To further examine this double-strand DNA repairing function of SMARCAD1 *in vivo*, I also examined two zebrafish mutants, SA1299 and p403. SA1299 carries a point mutation generated with ENU, and p403 is CRISPR-Cas9 small knockout mutant. One day post fertilized SA1299, p403, and wildtype embryos were treated with 15Gy X-ray irradiation then the expression level of γH2AX was examined at different time points. Approximate 50-100 fish embryos were pooled for protein collection at each time point. Similar to *in vitro* result, elevated γH2AX level was observed at all time points in both mutant embryos compared to wildtype. The reduction of γH2AX was delayed in two mutants after irradiation **(Figure 7B, C)**. These results confirmed my hypothesis that loss of function of *smarcad1a* compromises DNA damage repair in zebrafish.

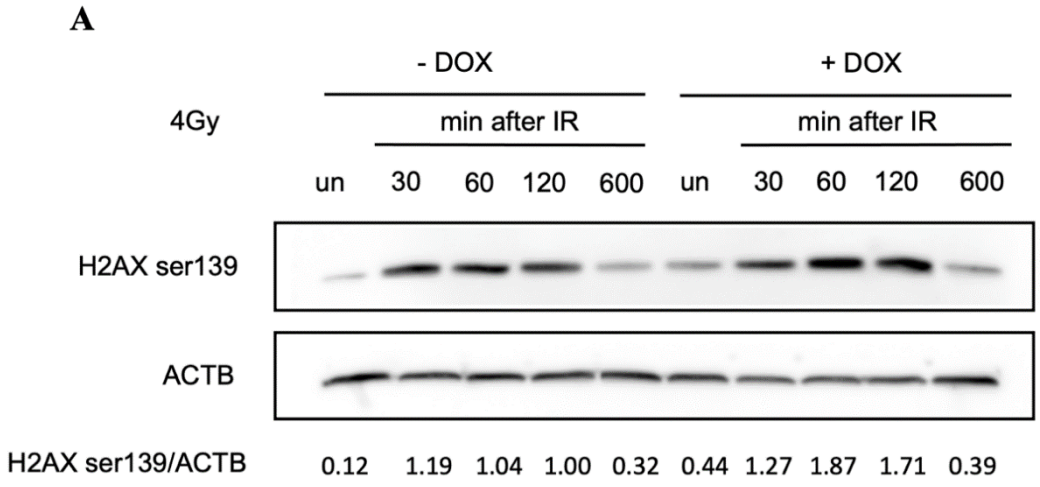

Figure 7. The Loss function of SMARCAD1 compromises DNA damage repair *in vitro* and *in vivo*. A) γH2AX expression was examined by western blot in CRISPR-Cas13d SMARCAD1 knockout HEI193 cell line after 4Gy X-ray irradiation. **B)** γH2AX expression was examined by western blot in wildtype, *smarcad1a*$^{sa1299-/-}$, and *smarcad1a*$^{p403-/-}$ 1dpf zebrafish embryos. **C)** Quantification of γH2AX expression measured by western blotting from A. Relative fold change of γH2AX were calculated upon each collecting time point after irradiation. Bars are the means of three independent experiments in same time point. Student's *t*-test was performed to caluate the significance between wildtype and two zebra fish mutants (SA1299 and p403) (*: $p \leq 0.05$; **: $p \leq 0.01$; ***: $p \leq 0.001$; NS: $p > 0.05$)

Figure 7 continued

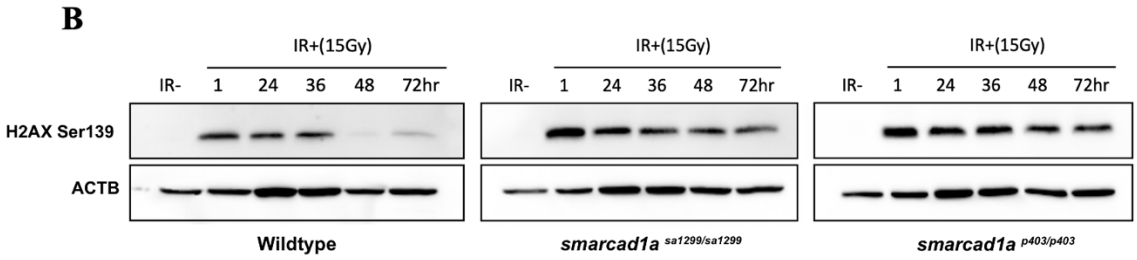

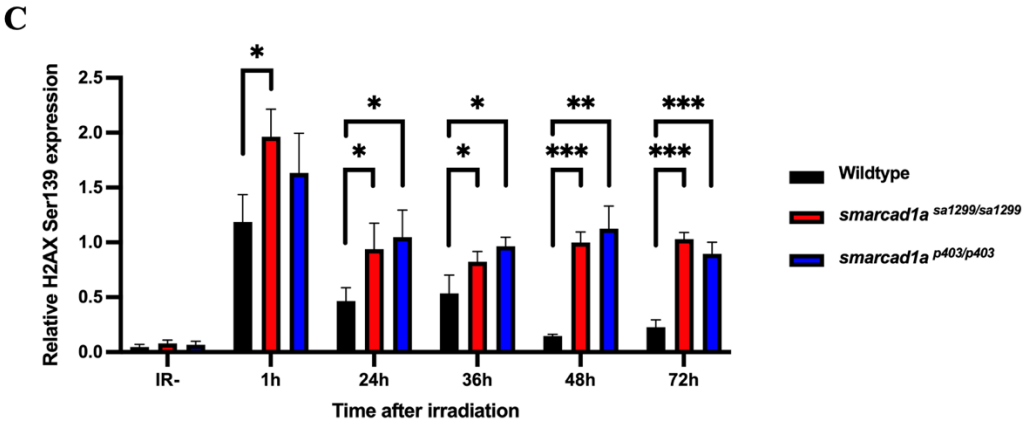

4. DISCUSSION

4.1 CRISPR-Cas13d is an efficient gene knockdown system

To study the tumor-suppressive function of *SMARCAD1* in human MPNST, I created a doxycycline-inducible SMARCAD1 knockdown Schwannoma cell line by CRISPR-Cas13d. Western blot was employed to examine the knockdown efficiency and sensitivity toward doxycycline treatment. The expression level of SMARCAD1 is significantly reduced after doxycycline treatment at a low concentration of doxycycline of 125ng/ml. **(Figure 5A)** This result indicates Tet-on CRISPR-Cas13d binary knockdown system efficiently knockdown SMARCAD1 in HEI193 cells. I also compared the sensitivity of Cas13d knockdown with a commercial shRNA (ULTRA-3351712) knockdown in the same Schwannoma cell line HEI193 **(Figure 5B)**. SMARCAD1 had not been significantly downregulated (around 60% reduction) until cells were treated with no less than 500ng/ml doxycycline. Compared to the shRNA knockdown cell line, the CRISPR-Cas13d cell line is more sensitive toward doxycycline treatment and has better efficiency of SMARCAD1 knockdown. This result is consistent with the previous discovery that CRISPR-Cas13d has better knockdown efficiency than shRNA, CRISPRi, and other types of Cas13s (Konermann et al., 2018). Although different knockdown efficiency between two cell lines might result from different constructs design or technical variances when generating stable cell lines with lentivirus. Our data have indicated that CRISPR-Cas13d is an efficient gene knockdown system, and it can be utilized in studying tumor drivers. However, the potential off-target effect of each gRNAs should be further evaluated.

4.2 Knockdown of SMARCAD1 causes cell growth inhibition

Several studies have linked *SMARCAD1* with cancer development together. Mutation of a skin-specific isoform of SMARCAD1 was found in quamous cell carcinoma patients (Günther et al., 2018). Homozygous *Etl1* (Mouse *SMARCAD1* ortholog) knockout mice experience serval abnormalities, including gastro-intestinal tumors (Schoor et al., 1999). SMARCAD1 knockdown was reported to cause a significant decrease in breast cancer cell growth (Al Kubaisy et al., 2016) and pancreatic cancer cells (Liu et al., 2019). Consistently, my knockdown experiment demonstrated that loss of function of *smarcad1* also leads to decreased cell proliferation and

anchorage-independent growth in schwannoma cell line HEI193 **(Figure 6A, B)**. Moreover, the loss of *smarcad1a*, one of the orthologs of human *SMARCAD1* in zebrafish, accelerates tumorigenesis of MPNST with *tp53* mutation background (Han et al., 2021). Although the growth inhibition is consistent in different cancer cell lines, this contrasts with the classical notion of tumor suppressor genes, whose loss of function usually promotes cell growth, such as TP53. It is worth noting that a recent result from our laboratory revealed that SMARCAD1 overexpression also caused cell growth inhibition (Han 2021). Thus, a proper expression level (gene dosage) of SMARCAD1 seems to be required for maintaining normal tissue and cells since this gene has been proved to have an essential function in heterochromatin formation, retroviral inhibition, and DNA damage repair.

4.3 SMARCAD1 involves in the DNA damage repair process

Our data shows knockdown of SMARCAD1 extents time of DSB marker γH2AX existing in X-ray irradiated human Schwannoma cells and zebrafish embryos **(Figure 7),** indicating the function of SMARCAD1 in DNA damage repairing mechanism. However, how SMARCAD1 involves in DNA damage repairing mechanisms is still unclear. Whether the reported mechanism remains the same in MPNSTs and is there other molecular mechanisms of *smarcad1* in DNA damage still need to be evaluated.

Tumor cells often experience more stress from double-strand break because, first, their hyperactivated cell replication induces more error during dysregulated mitosis (Ganem & Pellman, 2012). Second, genetic defects of the DNA damage repairing mechanism of tumor cells accumulate more damage (Torgovnick & Schumacher, 2015). This difference between normal cells and tumor cells can be a targetable characteristic for cancer therapy exampled by BRCA1 and BRCA2 mutants (Rose et al., 2020). Mutation of SMARCAD1 leads to PRAP inhibitor sensitivity in yeast and human osteosarcoma cell lines (Costelloe et al., 2012). Knockdown of SMARCAD1 was reported to increase the sensitivity of PRAP inhibitor in PRAPi resistant mouse breast tumor cells (Yu & Maria, 2021). Targeting SMARCAD1 combined with PRAP inhibition might provide potential target therapy for MNPST. Future studies could explore this possibility since currently there is no targeted therapy available for this type of malignant tumor.

REFERENCES

Abudayyeh, O. O., Gootenberg, J. S., Essletzbichler, P., Han, S., Joung, J., Belanto, J. J., Verdine, V., Cox, D. B. T., Kellner, M. J., Regev, A., Lander, E. S., Voytas, D. F., Ting, A. Y., & Zhang, F. (2017). RNA targeting with CRISPR-Cas13. *Nature*, *550*(7675), 280–284. https://doi.org/10.1038/nature24049

Adra, C. N., Donato, J.-L., Badovinac, R., Syed, F., Kheraj, R., Cai, H., Moran, C., Kolker, M. T., Turner, H., Weremowicz, S., Shirakawa, T., Morton, C. C., Schnipper, L. E., & Drews, R. (2000). SMARCAD1, a Novel Human Helicase Family-Defining Member Associated with Genetic Instability: Cloning, Expression, and Mapping to 4q22–q23, a Band Rich in Breakpoints and Deletion Mutants Involved in Several Human Diseases. *Genomics*, *69*(2), 162–173. https://doi.org/10.1006/geno.2000.6281

Al Kubaisy, E., Arafat, K., De Wever, O., Hassan, A. H., & Attoub, S. (2016). SMARCAD1 knockdown uncovers its role in breast cancer cell migration, invasion, and metastasis. *Expert Opinion on Therapeutic Targets*, *20*(9), 1035–1043. https://doi.org/10.1080/14728222.2016.1195059

Allison, K. H., Patel, R. M., Goldblum, J. R., & Rubin, B. P. (2005). Superficial Malignant Peripheral Nerve Sheath Tumor: A Rare and Challenging Diagnosis. *American Journal of Clinical Pathology*, *124*(5), 685–692. https://doi.org/10.1309/V8XMK5R78Q96V090

Amirian, E. S., Goodman, J. C., New, P., & Scheurer, M. E. (2014). Pediatric and adult malignant peripheral nerve sheath tumors: An analysis of data from the surveillance, epidemiology, and end results program. *Journal of Neuro-Oncology*, *116*(3), 609–616. https://doi.org/10.1007/s11060-013-1345-6

Angelov, L., Davis, A., O'Sullivan, B., Bell, R., & Guha, A. (1998). Neurogenic sarcomas: Experience at the University of Toronto. *Neurosurgery*, *43*(1), 56–64; discussion 64-65. https://doi.org/10.1097/00006123-199807000-00035

Aparicio, T., Baer, R., & Gautier, J. (2014). DNA double-strand break repair pathway choice and cancer. *DNA Repair*, *19*, 169–175. https://doi.org/10.1016/j.dnarep.2014.03.014

Baehring, J. M., Betensky, R. A., & Batchelor, T. T. (2003). Malignant peripheral nerve sheath tumor: The clinical spectrum and outcome of treatment. *Neurology*, *61*(5), 696–698. https://doi.org/10.1212/01.WNL.0000078813.05925.2C

Bates, J. E., Peterson, C. R., Dhakal, S., Giampoli, E. J., & Constine, L. S. (2014). Malignant peripheral nerve sheath tumors (MPNST): A SEER analysis of incidence across the age spectrum and therapeutic interventions in the pediatric population: Malignant Peripheral Nerve Sheath Tumors. *Pediatric Blood & Cancer*, *61*(11), 1955–1960. https://doi.org/10.1002/pbc.25149

Beert, E., Brems, H., Daniëls, B., De Wever, I., Van Calenbergh, F., Schoenaers, J., Debiec-Rychter, M., Gevaert, O., De Raedt, T., Van Den Bruel, A., de Ravel, T., Cichowski, K., Kluwe, L., Mautner, V., Sciot, R., & Legius, E. (2011). Atypical neurofibromas in neurofibromatosis type 1 are premalignant tumors. *Genes, Chromosomes and Cancer*, *50*(12), 1021–1032. https://doi.org/10.1002/gcc.20921

Berghmans, S., Murphey, R. D., Wienholds, E., Neuberg, D., Kutok, J. L., Fletcher, C. D. M., Morris, J. P., Liu, T. X., Schulte-Merker, S., Kanki, J. P., Plasterk, R., Zon, L. I., & Look, A. T. (2005). Tp53 mutant zebrafish develop malignant peripheral nerve sheath tumors. *Proceedings of the National Academy of Sciences*, *102*(2), 407–412. https://doi.org/10.1073/pnas.0406252102

Bergoug, M., Doudeau, M., Godin, F., Mosrin, C., Vallée, B., & Bénédetti, H. (2020). Neurofibromin Structure, Functions and Regulation. *Cells*, *9*(11), 2365. https://doi.org/10.3390/cells9112365

Bernstein, E., Caudy, A. A., Hammond, S. M., & Hannon, G. J. (2001). Role for a bidentate ribonuclease in the initiation step of RNA interference. *Nature*, *409*(6818), 363–366. https://doi.org/10.1038/35053110

Bradford, D., & Kim, A. (2015). Current treatment options for malignant peripheral nerve sheath tumors. *Current Treatment Options in Oncology*, *16*(3), 328. https://doi.org/10.1007/s11864-015-0328-6

Brummelkamp, T. R., Bernards, R., & Agami, R. (2002). A system for stable expression of short interfering RNAs in mammalian cells. *Science (New York, N.Y.)*, *296*(5567), 550–553. https://doi.org/10.1126/science.1068999

Cetin, E., Cengiz, B., Gunduz, E., Gunduz, M., Nagatsuka, H., Bekir-Beder, L., Fukushima, K., Pehlivan, D., N, M. O., Nishizaki, K., Shimizu, K., & Nagai, N. (2008). Deletion mapping of chromosome 4q22-35 and identification of four frequently deleted regions in head and neck cancers. *Neoplasma*, *55*(4), 299–304.

Chakraborty, S., Pandita, R. K., Hambarde, S., Mattoo, A. R., Charaka, V., Ahmed, K. M., Iyer, S. P., Hunt, C. R., & Pandita, T. K. (2018). SMARCAD1 Phosphorylation and Ubiquitination Are Required for Resection during DNA Double-Strand Break Repair. *IScience*, *2*, 123–135. https://doi.org/10.1016/j.isci.2018.03.016

Chaney, K. E., Perrino, M. R., Kershner, L. J., Patel, A. V., Wu, J., Choi, K., Rizvi, T. A., Dombi, E., Szabo, S., Largaespada, D. A., & Ratner, N. (2020). Cdkn2a Loss in a Model of Neurofibroma Demonstrates Stepwise Tumor Progression to Atypical Neurofibroma and MPNST. *Cancer Research*, *80*(21), 4720–4730. https://doi.org/10.1158/0008-5472.CAN-19-1429

Chen, X., Cui, D., Papusha, A., Zhang, X., Chu, C.-D., Tang, J., Chen, K., Pan, X., & Ira, G. (2012). The Fun30 nucleosome remodeller promotes resection of DNA double-strand break ends. *Nature*, *489*(7417), 576–580. https://doi.org/10.1038/nature11355

Cleven, A. H. G., Sannaa, G. A. A., Briaire-de Bruijn, I., Ingram, D. R., van de Rijn, M., Rubin, B. P., de Vries, M. W., Watson, K. L., Torres, K. E., Wang, W.-L., van Duinen, S. G., Hogendoorn, P. C. W., Lazar, A. J., & Bovée, J. V. M. G. (2016). Loss of H3K27 tri-methylation is a diagnostic marker for malignant peripheral nerve sheath tumors and an indicator for an inferior survival. *Modern Pathology*, *29*(6), 582–590. https://doi.org/10.1038/modpathol.2016.45

Combemale, P., Valeyrie-Allanore, L., Giammarile, F., Pinson, S., Guillot, B., Goulart, D. M., Wolkenstein, P., Blay, J. Y., & Mognetti, T. (2014). Utility of 18F-FDG PET with a Semi-Quantitative Index in the Detection of Sarcomatous Transformation in Patients with Neurofibromatosis Type 1. *PLoS ONE*, *9*(2), e85954. https://doi.org/10.1371/journal.pone.0085954

Cong, L., Ran, F. A., Cox, D., Lin, S., Barretto, R., Habib, N., Hsu, P. D., Wu, X., Jiang, W., Marraffini, L. A., & Zhang, F. (2013). Multiplex Genome Engineering Using CRISPR/Cas Systems. *Science*, *339*(6121), 819–823. https://doi.org/10.1126/science.1231143

Costelloe, T., Louge, R., Tomimatsu, N., Mukherjee, B., Martini, E., Khadaroo, B., Dubois, K., Wiegant, W. W., Thierry, A., Burma, S., van Attikum, H., & Llorente, B. (2012). The yeast Fun30 and human SMARCAD1 chromatin remodellers promote DNA end resection. *Nature*, *489*(7417), 581–584. https://doi.org/10.1038/nature11353

Czarnecka, A. M., Sobczuk, P., Zdzienicki, M., Spalek, M., Rutkowsko, P. (2018). Malignant peripheral nerve sheath tumour (MPNST). *Oncology in Clinical Practice, 14*(6), 13. http://doi.org/10.5603/OCP.2018.0050

De Raedt, T., Beert, E., Pasmant, E., Luscan, A., Brems, H., Ortonne, N., Helin, K., Hornick, J. L., Mautner, V., Kehrer-Sawatzki, H., Clapp, W., Bradner, J., Vidaud, M., Upadhyaya, M., Legius, E., & Cichowski, K. (2014). PRC2 loss amplifies Ras-driven transcription and confers sensitivity to BRD4-based therapies. *Nature*, *514*(7521), 247–251. https://doi.org/10.1038/nature13561

Densham, R. M., Garvin, A. J., Stone, H. R., Strachan, J., Baldock, R. A., Daza-Martin, M., Fletcher, A., Blair-Reid, S., Beesley, J., Johal, B., Pearl, L. H., Neely, R., Keep, N. H., Watts, F. Z., & Morris, J. R. (2016). Human BRCA1–BARD1 ubiquitin ligase activity counteracts chromatin barriers to DNA resection. *Nature Structural & Molecular Biology*, *23*(7), 647–655. https://doi.org/10.1038/nsmb.3236

Doiguchi, M., Nakagawa, T., Imamura, Y., Yoneda, M., Higashi, M., Kubota, K., Yamashita, S., Asahara, H., Iida, M., Fujii, S., Ikura, T., Liu, Z., Nandu, T., Kraus, W. L., Ueda, H., & Ito, T. (2016). SMARCAD1 is an ATP-dependent stimulator of nucleosomal H2A acetylation via CBP, resulting in transcriptional regulation. *Scientific Reports*, *6*, 20179. https://doi.org/10.1038/srep20179

Du, P., Zhu, J., Zhang, Z.-D., He, C., Ye, M.-Y., Liu, Y.-X., Tian, Q.-H., & Zeng, J.-S. (2019). Recurrent epithelioid malignant peripheral nerve sheath tumor with neurofibromatosis type 1: A case report and literature review. *Oncology Letters*, *18*(3), 3072–3080. https://doi.org/10.3892/ol.2019.10676

Evans, D. G. R., Birch, J. M., Ramsden, R. T., Sharif, S., & Baser, M. E. (2006). Malignant transformation and new primary tumours after therapeutic radiation for benign disease: Substantial risks in certain tumour prone syndromes. *Journal of Medical Genetics*, *43*(4), 289–294. https://doi.org/10.1136/jmg.2005.036319

Farid, M., Demicco, E. G., Garcia, R., Ahn, L., Merola, P. R., Cioffi, A., & Maki, R. G. (2014). Malignant Peripheral Nerve Sheath Tumors. *The Oncologist*, *19*(2), 193–201. https://doi.org/10.1634/theoncologist.2013-0328

Faucherre, A., Taylor, G. S., Overvoorde, J., Dixon, J. E., & Hertog, J. den. (2008). Zebrafish pten genes have overlapping and non-redundant functions in tumorigenesis and embryonic development. *Oncogene*, *27*(8), 1079–1086. https://doi.org/10.1038/sj.onc.1210730

Ferrari, A., Bisogno, G., & Carli, M. (2007). Management of Childhood Malignant Peripheral Nerve Sheath Tumor. *Pediatric Drugs*, *9*(4), 239–248. https://doi.org/10.2165/00148581-200709040-00005

Ferrari, A., Casanova, M., Bisogno, G., Mattke, A., Meazza, C., Gandola, L., Sotti, G., Cecchetto, G., Harms, D., Koscielniak, E., Treuner, J., & Carli, M. (2002). Clear cell sarcoma of tendons and aponeuroses in pediatric patients. *Cancer*, *94*(12), 3269–3276. https://doi.org/10.1002/cncr.10597

Fradet-Turcotte, A., Canny, M. D., Escribano-Díaz, C., Orthwein, A., Leung, C. C. Y., Huang, H., Landry, M.-C., Kitevski-LeBlanc, J., Noordermeer, S. M., Sicheri, F., & Durocher, D. (2013). 53BP1 is a reader of the DNA-damage-induced H2A Lys 15 ubiquitin mark. *Nature*, *499*(7456), 50–54. https://doi.org/10.1038/nature12318

Fuchs, B., Spinner, R. J., & Rock, M. G. (2005). Malignant peripheral nerve sheath tumors: An update. *Journal of Surgical Orthopaedic Advances*, *14*(4), 168–174.

Ganem, N. J., & Pellman, D. (2012). Linking abnormal mitosis to the acquisition of DNA damage. *Journal of Cell Biology*, *199*(6), 871–881. https://doi.org/10.1083/jcb.201210040

Gregorian, C., Nakashima, J., Dry, S. M., Nghiemphu, P. L., Smith, K. B., Ao, Y., Dang, J., Lawson, G., Mellinghoff, I. K., Mischel, P. S., Phelps, M., Parada, L. F., Liu, X., Sofroniew, M. V., Eilber, F. C., & Wu, H. (2009). PTEN dosage is essential for neurofibroma development and malignant transformation. *Proceedings of the National Academy of Sciences of the United States of America*, *106*(46), 19479–19484. https://doi.org/10.1073/pnas.0910398106

Günther, C., Lee-Kirsch, M. A., Eckhard, J., Matanovic, A., Kerscher, T., Rüschendorf, F., Klein, B., Berndt, N., Zimmermann, N., Flachmeier, C., Thuß, T., Lucas, N., Marenholz, I., Esparza-Gordillo, J., Hübner, N., Traupe, H., Delaporte, E., & Lee, Y.-A. (2018). SMARCAD1 Haploinsufficiency Underlies Huriez Syndrome and Associated Skin Cancer Susceptibility. *The Journal of Investigative Dermatology*, *138*(6), 1428–1431. https://doi.org/10.1016/j.jid.2018.01.015

Han, H., Jiang, G., Kumari, R., Silic, M. R., Owens, J. L., Hu, C., Mittal, S. K., & Zhang, G. (2021). Loss of smarcad1a accelerates tumorigenesis of malignant peripheral nerve sheath tumors in zebrafish. *Genes, Chromosomes and Cancer*, *60*(11), 743–761. https://doi.org/10.1002/gcc.22983

Hanahan, D. (1983). Studies on transformation of Escherichia coli with plasmids. *Journal of Molecular Biology*, *166*(4), 557–580. https://doi.org/10.1016/S0022-2836(83)80284-8

Higham, C. S., Steinberg, S. M., Dombi, E., Perry, A., Helman, L. J., Schuetze, S. M., Ludwig, J. A., Staddon, A., Milhem, M. M., Rushing, D., Jones, R. L., Livingston, M., Goldman, S., Moertel, C., Wagner, L., Janhofer, D., Annunziata, C. M., Reinke, D., Long, L., … Widemann, B. C. (2017). SARC006: Phase II Trial of Chemotherapy in Sporadic and Neurofibromatosis Type 1 Associated Chemotherapy-Naive Malignant Peripheral Nerve Sheath Tumors. *Sarcoma*, *2017*, 1–8. https://doi.org/10.1155/2017/8685638

Hsu, P. D., Lander, E. S., & Zhang, F. (2014). Development and Applications of CRISPR-Cas9 for Genome Engineering. *Cell*, *157*(6), 1262–1278. https://doi.org/10.1016/j.cell.2014.05.010

Inoue, T., Kuwashiro, M., Misago, N., & Narisawa, Y. (2014). Superficial malignant peripheral nerve sheath tumor arising from diffuse neurofibroma in a neurofibromatosis type 1 patient. *The Journal of Dermatology*, *41*(7), 631–633. https://doi.org/10.1111/1346-8138.12536

Kar, M., Deo, S. V. S., Shukla, N. K., Malik, A., DattaGupta, S., Mohanti, B. K., & Thulkar, S. (2006). Malignant peripheral nerve sheath tumors (MPNST) – Clinicopathological study and treatment outcome of twenty-four cases. *World Journal of Surgical Oncology*, *4*(1), 55. https://doi.org/10.1186/1477-7819-4-55

Kivlin, C. M., Watson, K. L., Al Sannaa, G. A., Belousov, R., Ingram, D. R., Huang, K.-L., May, C. D., Bolshakov, S., Landers, S. M., Kalam, A. A., Slopis, J. M., McCutcheon, I. E., Pollock, R. E., Lev, D., Lazar, A. J., & Torres, K. E. (2016). Poly (ADP) ribose polymerase inhibition: A potential treatment of malignant peripheral nerve sheath tumor. *Cancer Biology & Therapy*, *17*(2), 129–138. https://doi.org/10.1080/15384047.2015.1108486

Knight, S. W. E., Knight, T. E., Santiago, T., Murphy, A. J., & Abdelhafeez, A. H. (2022). Malignant Peripheral Nerve Sheath Tumors—A Comprehensive Review of Pathophysiology, Diagnosis, and Multidisciplinary Management. *Children*, *9*(1), 38. https://doi.org/10.3390/children9010038

Konermann, S., Lotfy, P., Brideau, N. J., Oki, J., Shokhirev, M. N., & Hsu, P. D. (2018). Transcriptome Engineering with RNA-Targeting Type VI-D CRISPR Effectors. *Cell*, *173*(3), 665-676.e14. https://doi.org/10.1016/j.cell.2018.02.033

Kuberappa, P. H. (2016). Certainty of S100 from Physiology to Pathology. *JOURNAL OF CLINICAL AND DIAGNOSTIC RESEARCH*. https://doi.org/10.7860/JCDR/2016/17949.8022

Le Guellec, S., Macagno, N., Velasco, V., Lamant, L., Lae, M., Filleron, T., Malissen, N., Cassagnau, E., Terrier, P., Chevreau, C., Ranchere-Vince, D., & Coindre, J.-M. (2017). Loss of H3K27 trimethylation is not suitable for distinguishing malignant peripheral nerve sheath tumor from melanoma: A study of 387 cases including mimicking lesions. *Modern Pathology*, *30*(12), 1677–1687. https://doi.org/10.1038/modpathol.2017.91

Lee, J., Shik Choi, E., David Seo, H., Kang, K., Gilmore, J. M., Florens, L., Washburn, M. P., Choe, J., Workman, J. L., & Lee, D. (2017). Chromatin remodeller Fun30Fft3 induces nucleosome disassembly to facilitate RNA polymerase II elongation. *Nature Communications*, *8*(1), 14527. https://doi.org/10.1038/ncomms14527

Legius, E., Dierick, H., Wu, R., Hall, B. K., Marynen, P., Cassiman, J.-J., & Glover, T. W. (1994). TP53 mutations are frequent in malignant NFI tumors. *Genes, Chromosomes and Cancer*, *10*(4), 250–255. https://doi.org/10.1002/gcc.2870100405

Liu, F., Xia, Z., Zhang, M., Ding, J., Feng, Y., Wu, J., Dong, Y., Gao, W., Han, Z., Liu, Y., Yao, Y., & Li, D. (2019). SMARCAD1 Promotes Pancreatic Cancer Cell Growth and Metastasis through Wnt/β-catenin-Mediated EMT. *International Journal of Biological Sciences*, *15*(3), 636–646. https://doi.org/10.7150/ijbs.29562

Louis, D. N., Perry, A., Reifenberger, G., von Deimling, A., Figarella-Branger, D., Cavenee, W. K., Ohgaki, H., Wiestler, O. D., Kleihues, P., & Ellison, D. W. (2016). The 2016 World Health Organization Classification of Tumors of the Central Nervous System: A summary. *Acta Neuropathologica*, *131*(6), 803–820. https://doi.org/10.1007/s00401-016-1545-1

Mah, L.-J., El-Osta, A., & Karagiannis, T. C. (2010). γH2AX: A sensitive molecular marker of DNA damage and repair. *Leukemia*, *24*(4), 679–686. https://doi.org/10.1038/leu.2010.6

Makarova, K. S., Wolf, Y. I., Alkhnbashi, O. S., Costa, F., Shah, S. A., Saunders, S. J., Barrangou, R., Brouns, S. J. J., Charpentier, E., Haft, D. H., Horvath, P., Moineau, S., Mojica, F. J. M., Terns, R. M., Terns, M. P., White, M. F., Yakunin, A. F., Garrett, R. A., van der Oost, J., … Koonin, E. V. (2015). An updated evolutionary classification of CRISPR–Cas systems. *Nature Reviews Microbiology*, *13*(11), 722–736. https://doi.org/10.1038/nrmicro3569

Maki, R. G., D'Adamo, D. R., Keohan, M. L., Saulle, M., Schuetze, S. M., Undevia, S. D., Livingston, M. B., Cooney, M. M., Hensley, M. L., Mita, M. M., Takimoto, C. H., Kraft, A. S., Elias, A. D., Brockstein, B., Blachère, N. E., Edgar, M. A., Schwartz, L. H., Qin, L.-X., Antonescu, C. R., & Schwartz, G. K. (2009). Phase II Study of Sorafenib in Patients With Metastatic or Recurrent Sarcomas. *Journal of Clinical Oncology*, *27*(19), 3133–3140. https://doi.org/10.1200/JCO.2008.20.4495

Mantripragada, K. K., de Ståhl, T. D., Patridge, C., Menzel, U., Andersson, R., Chuzhanova, N., Kluwe, L., Guha, A., Mautner, V., Dumanski, J. P., & Upadhyaya, M. (2009). Genome-wide high-resolution analysis of DNA copy number alterations in NF1-associated malignant peripheral nerve sheath tumors using 32K BAC array. *Genes, Chromosomes and Cancer*, *48*(10), 897–907. https://doi.org/10.1002/gcc.20695

Markert, J., Zhou, K., & Luger, K. (2021). SMARCAD1 is an ATP-dependent histone octamer exchange factor with de novo nucleosome assembly activity. *Science Advances*, *7*(42), eabk2380. https://doi.org/10.1126/sciadv.abk2380

Martin, G. A., Viskoohil, D., Bollag, G., McCabe, P. C., Crosier, W. J., Haubruck, H., Conroy, L., Clark, R., O'Connell, P., Cawthon, R. M., Innis, M. A., & McCormick, F. (1990). The GAP-related domain of the neurofibromatosis type 1 gene product interacts with ras p21. *Cell*, *63*(4), 843–849. https://doi.org/10.1016/0092-8674(90)90150-D

Mattingly, R. R., Kraniak, J. M., Dilworth, J. T., Mathieu, P., Bealmear, B., Nowak, J. E., Benjamins, J. A., Tainsky, M. A., & Reiners, J. J. (2006). The mitogen-activated protein kinase/extracellular signal-regulated kinase kinase inhibitor PD184352 (CI-1040) selectively induces apoptosis in malignant schwannoma cell lines. *The Journal of Pharmacology and Experimental Therapeutics*, *316*(1), 456–465. https://doi.org/10.1124/jpet.105.091454

Miettinen, M., McCue, P. A., Sarlomo-Rikala, M., Biernat, W., Czapiewski, P., Kopczynski, J., Thompson, L. D., Lasota, J., Wang, Z., & Fetsch, J. F. (2015). Sox10—A Marker for Not Only Schwannian and Melanocytic Neoplasms But Also Myoepithelial Cell Tumors of Soft Tissue: A Systematic Analysis of 5134 Tumors. *American Journal of Surgical Pathology*, *39*(6), 826–835. https://doi.org/10.1097/PAS.0000000000000398

Mohanraju, P., Makarova, K. S., Zetsche, B., Zhang, F., Koonin, E. V., & van der Oost, J. (2016). Diverse evolutionary roots and mechanistic variations of the CRISPR-Cas systems. *Science*, *353*(6299), aad5147. https://doi.org/10.1126/science.aad5147

Naber, U., Friedrich, R. E., Glatzel, M., Mautner, V. F., & Hagel, C. (2011). Podoplanin and CD34 in peripheral nerve sheath tumours: Focus on neurofibromatosis 1-associated atypical neurofibroma. *Journal of Neuro-Oncology*, *103*(2), 239–245. https://doi.org/10.1007/s11060-010-0385-4

Natalie Wu, L. M., & Lu, Q. R. (2019). Therapeutic targets for malignant peripheral nerve sheath tumors. *Future Neurology*, *14*(1), FNL7. https://doi.org/10.2217/fnl-2018-0026

Niu, Q., Wang, W., Wei, Z., Byeon, B., Das, A. B., Chen, B.-S., & Wu, W.-H. (2020). Role of the ATP-dependent chromatin remodeling enzyme Fun30/Smarcad1 in the regulation of mRNA splicing. *Biochemical and Biophysical Research Communications*, *526*(2), 453–458. https://doi.org/10.1016/j.bbrc.2020.02.175

Nykänen, A., Haley, B., & Zamore, P. D. (2001). ATP requirements and small interfering RNA structure in the RNA interference pathway. *Cell*, *107*(3), 309–321. https://doi.org/10.1016/s0092-8674(01)00547-5

O'Connell, M. R. (2019). Molecular Mechanisms of RNA Targeting by Cas13-containing Type VI CRISPR-Cas Systems. *Journal of Molecular Biology*, *431*(1), 66–87. https://doi.org/10.1016/j.jmb.2018.06.029

Perry, A., Kunz, S. N., Fuller, C. E., Banerjee, R., Marley, E. F., Liapis, H., Watson, M. A., & Gutmann, D. H. (2002). Differential *NF1* , *p16* , and *EGFR* Patterns by Interphase Cytogenetics (FISH) in Malignant Peripheral Nerve Sheath Tumor (MPNST) and Morphologically Similar Spindle Cell Neoplasms. *Journal of Neuropathology & Experimental Neurology*, *61*(8), 702–709. https://doi.org/10.1093/jnen/61.8.702

Postlethwait, J. H., Yan, Y. L., Gates, M. A., Horne, S., Amores, A., Brownlie, A., Donovan, A., Egan, E. S., Force, A., Gong, Z., Goutel, C., Fritz, A., Kelsh, R., Knapik, E., Liao, E., Paw, B., Ransom, D., Singer, A., Thomson, M., … Talbot, W. S. (1998). Vertebrate genome evolution and the zebrafish gene map. *Nature Genetics*, *18*(4), 345–349. https://doi.org/10.1038/ng0498-345

Prieto-Granada, C. N., Wiesner, T., Messina, J. L., Jungbluth, A. A., Chi, P., & Antonescu, C. R. (2016). Loss of H3K27me3 Expression Is a Highly Sensitive Marker for Sporadic and Radiation-induced MPNST. *The American Journal of Surgical Pathology*, *40*(4), 479–489. https://doi.org/10.1097/PAS.0000000000000564

Prudner, B. C., Ball, T., Rathore, R., & Hirbe, A. C. (2020). Diagnosis and management of malignant peripheral nerve sheath tumors: Current practice and future perspectives. *Neuro-Oncology Advances*, *2*(Supplement_1), i40–i49. https://doi.org/10.1093/noajnl/vdz047

Putzbach, W., Gao, Q. Q., Patel, M., van Dongen, S., Haluck-Kangas, A., Sarshad, A. A., Bartom, E. T., Kim, K.-Y. A., Scholtens, D. M., Hafner, M., Zhao, J. C., Murmann, A. E., & Peter, M. E. (2017). Many si/shRNAs can kill cancer cells by targeting multiple survival genes through an off-target mechanism. *ELife*, *6*, e29702. https://doi.org/10.7554/eLife.29702

Rodriguez, F. J., Folpe, A. L., Giannini, C., & Perry, A. (2012). Pathology of peripheral nerve sheath tumors: Diagnostic overview and update on selected diagnostic problems. *Acta Neuropathologica*, *123*(3), 295–319. https://doi.org/10.1007/s00401-012-0954-z

Rose, M., Burgess, J. T., O'Byrne, K., Richard, D. J., & Bolderson, E. (2020). PARP Inhibitors: Clinical Relevance, Mechanisms of Action and Tumor Resistance. *Frontiers in Cell and Developmental Biology*, *8*. https://www.frontiersin.org/article/10.3389/fcell.2020.564601

Rowbotham, S. P., Barki, L., Neves-Costa, A., Santos, F., Dean, W., Hawkes, N., Choudhary, P., Will, W. R., Webster, J., Oxley, D., Green, C. M., Varga-Weisz, P., & Mermoud, J. E. (2011). Maintenance of Silent Chromatin through Replication Requires SWI/SNF-like Chromatin Remodeler SMARCAD1. *Molecular Cell*, *42*(3), 285–296. https://doi.org/10.1016/j.molcel.2011.02.036

Rudner, L. A., Brown, K. H., Dobrinski, K. P., Bradley, D. F., Garcia, M. I., Smith, A. C. H., Downie, J. M., Meeker, N. D., Look, A. T., Downing, J. R., Gutierrez, A., Mullighan, C. G., Schiffman, J. D., Lee, C., Trede, N. S., & Frazer, J. K. (2011). Shared acquired genomic changes in zebrafish and human T-ALL. *Oncogene*, *30*(41), 4289–4296. https://doi.org/10.1038/onc.2011.138

Sachs, P., Ding, D., Bergmaier, P., Lamp, B., Schlagheck, C., Finkernagel, F., Nist, A., Stiewe, T., & Mermoud, J. E. (2019). SMARCAD1 ATPase activity is required to silence endogenous retroviruses in embryonic stem cells. *Nature Communications*, *10*. https://doi.org/10.1038/s41467-019-09078-0

Schoor, M., Schuster-Gossler, K., Roopenian, D., & Gossler, A. (1999). Skeletal dysplasias, growth retardation, reduced postnatal survival, and impaired fertility in mice lacking the SNF2/SWI2 family member ETL1. *Mechanisms of Development*, *85*(1–2), 73–83. https://doi.org/10.1016/S0925-4773(99)00090-8

Seno, N., Fukushima, T., Gomi, D., Kobayashi, T., Sekiguchi, N., Matsushita, H., Ozawa, T., Tsukahara, Y., Mamiya, K., Koizumi, T., & Sano, K. (2017). Successful treatment with doxorubicin and ifosfamide for mediastinal malignant peripheral nerve sheath tumor with loss of H3K27me3 expression. *Thoracic Cancer*, *8*(6), 720–723. https://doi.org/10.1111/1759-7714.12498

Shin, J., Padmanabhan, A., de Groh, E. D., Lee, J.-S., Haidar, S., Dahlberg, S., Guo, F., He, S., Wolman, M. A., Granato, M., Lawson, N. D., Wolfe, S. A., Kim, S.-H., Solnica-Krezel, L., Kanki, J. P., Ligon, K. L., Epstein, J. A., & Look, A. T. (2012). Zebrafish neurofibromatosis type 1 genes have redundant functions in tumorigenesis and embryonic development. *Disease Models & Mechanisms*, *5*(6), 881–894. https://doi.org/10.1242/dmm.009779

Shmakov, S., Smargon, A., Scott, D., Cox, D., Pyzocha, N., Yan, W., Abudayyeh, O. O., Gootenberg, J. S., Makarova, K. S., Wolf, Y. I., Severinov, K., Zhang, F., & Koonin, E. V. (2017). Diversity and evolution of class 2 CRISPR–Cas systems. *Nature Reviews Microbiology*, *15*(3), 169–182. https://doi.org/10.1038/nrmicro.2016.184

Skotheim, R. I., Kallioniemi, A., Bjerkhagen, B., Mertens, F., Brekke, H. R., Monni, O., Mousses, S., Mandahl, N., Soeter, G., Nesland, J. M., Smeland, S., Kallioniemi, O.-P., & Lothe, R. A. (2003). Topoisomerase-II alpha is upregulated in malignant peripheral nerve sheath tumors and associated with clinical outcome. *Journal of Clinical Oncology: Official Journal of the American Society of Clinical Oncology*, *21*(24), 4586–4591. https://doi.org/10.1200/JCO.2003.07.067

Stasik, C. J., & Tawfik, O. (2006). Malignant Peripheral Nerve Sheath Tumor With Rhabdomyosarcomatous Differentiation (Malignant Triton Tumor). *Archives of Pathology & Laboratory Medicine*, *130*(12), 1878–1881. https://doi.org/10.5858/2006-130-1878-MPNSTW

Sugita, S., Aoyama, T., Emori, M., Kido, T., Takenami, T., Sakuraba, K., Terai, K., Sugawara, T., Tsujiwaki, M., & Hasegawa, T. (2021). Assessment of H3K27me3 immunohistochemistry and combination of NF1 and p16 deletions by fluorescence in situ hybridization in the differential diagnosis of malignant peripheral nerve sheath tumor and its histological mimics. *Diagnostic Pathology*, *16*(1), 79. https://doi.org/10.1186/s13000-021-01140-0

Terui, R., Nagao, K., Kawasoe, Y., Taki, K., Higashi, T. L., Tanaka, S., Nakagawa, T., Obuse, C., Masukata, H., & Takahashi, T. S. (2018). Nucleosomes around a mismatched base pair are excluded via an Msh2-dependent reaction with the aid of SNF2 family ATPase Smarcad1. *Genes & Development*, *32*(11–12), 806–821. https://doi.org/10.1101/gad.310995.117

Thway, K., & Fisher, C. (2014). Malignant peripheral nerve sheath tumor: Pathology and genetics. *Annals of Diagnostic Pathology*, *18*(2), 109–116. https://doi.org/10.1016/j.anndiagpath.2013.10.007

Torgovnick, A., & Schumacher, B. (2015). DNA repair mechanisms in cancer development and therapy. *Frontiers in Genetics*, *6*. https://doi.org/10.3389/fgene.2015.00157

Uzunoglu, F. G., Dethlefsen, E., Hanssen, A., Wrage, M., Deutsch, L., Harms-Effenberger, K., Vashist, Y. K., Reeh, M., Sauter, G., Simon, R., Bockhorn, M., Pantel, K., Izbicki, J. R., & Wikman, H. (2014). Loss of 4q21.23-22.1 Is a Prognostic Marker for Disease Free and Overall Survival in Non-Small Cell Lung Cancer. *PLoS ONE*, *9*(12), e113315. https://doi.org/10.1371/journal.pone.0113315

Wessels, H.-H., Méndez-Mancilla, A., Guo, X., Legut, M., Daniloski, Z., & Sanjana, N. E. (2020). Massively parallel Cas13 screens reveal principles for guide RNA design. *Nature Biotechnology*, *38*(6), 722–727. https://doi.org/10.1038/s41587-020-0456-9

Widemann, B. C., Salzer, W. L., Arceci, R. J., Blaney, S. M., Fox, E., End, D., Gillespie, A., Whitcomb, P., Palumbo, J. S., Pitney, A., Jayaprakash, N., Zannikos, P., & Balis, F. M. (2006). Phase I Trial and Pharmacokinetic Study of the Farnesyltransferase Inhibitor Tipifarnib in Children With Refractory Solid Tumors or Neurofibromatosis Type I and Plexiform Neurofibromas. *Journal of Clinical Oncology*, *24*(3), 507–516. https://doi.org/10.1200/JCO.2005.03.8638

Wilson, M. D., Benlekbir, S., Fradet-Turcotte, A., Sherker, A., Julien, J.-P., McEwan, A., Noordermeer, S. M., Sicheri, F., Rubinstein, J. L., & Durocher, D. (2016). The structural basis of modified nucleosome recognition by 53BP1. *Nature*, *536*(7614), 100–103. https://doi.org/10.1038/nature18951

Wright, A. V., Nuñez, J. K., & Doudna, J. A. (2016). Biology and Applications of CRISPR Systems: Harnessing Nature's Toolbox for Genome Engineering. *Cell*, *164*(1–2), 29–44. https://doi.org/10.1016/j.cell.2015.12.035

Yang, F.-C., Ingram, D. A., Chen, S., Zhu, Y., Yuan, J., Li, X., Yang, X., Knowles, S., Horn, W., Li, Y., Zhang, S., Yang, Y., Vakili, S. T., Yu, M., Burns, D., Robertson, K., Hutchins, G., Parada, L. F., & Clapp, D. W. (2008). Nf1-Dependent Tumors Require a Microenvironment Containing Nf1+/−- and c-kit-Dependent Bone Marrow. *Cell*, *135*(3), 437–448. https://doi.org/10.1016/j.cell.2008.08.041

Yu, C. S., & Maria, E. (2021). SMARCAD1-mediated active replication fork stability maintains genome integrity. *SCIENCE ADVANCES*, 20.

Zhang, G., Hoersch, S., Amsterdam, A., Whittaker, C. A., Beert, E., Catchen, J. M., Farrington, S., Postlethwait, J. H., Legius, E., Hopkins, N., & Lees, J. A. (2013). Comparative Oncogenomic Analysis of Copy Number Alterations in Human and Zebrafish Tumors Enables Cancer Driver Discovery. *PLoS Genetics*, *9*(8), e1003734. https://doi.org/10.1371/journal.pgen.1003734

Zhang, M., Wang, Y., Jones, S., Sausen, M., McMahon, K., Sharma, R., Wang, Q., Belzberg, A. J., Chaichana, K., Gallia, G. L., Gokaslan, Z. L., Riggins, G. J., Wolinksy, J.-P., Wood, L. D., Montgomery, E. A., Hruban, R. H., Kinzler, K. W., Papadopoulos, N., Vogelstein, B., & Bettegowda, C. (2014). Somatic mutations of SUZ12 in malignant peripheral nerve sheath tumors. *Nature Genetics*, *46*(11), 1170–1172. https://doi.org/10.1038/ng.3116